Catalysis Science & Technology

Accepted Manuscript

This article can be cited before page numbers have been issued, to do this please use: R. González-Fernández, D. Álvarez, P. Crochet, V. Cadierno, M. I. Menendez and R. López, *Catal. Sci. Technol.*, 2020, DOI: 10.1039/D0CY00523A.

ROYAL SOCIETY OF CHEMISTRY

rsc.li/catalysis

View Article Online
DOI: 10.1039/D0CY00523A

ARTICLE

Catalytic hydration of cyanamides with phosphinous acid-based ruthenium(II) and osmium(II) complexes: Scope and mechanistic insights

Received 00th January 20xx,
Accepted 00th January 20xx

DOI: 10.1039/x0xx00000x

Rebeca González-Fernández,[a] Daniel Álvarez,[b] Pascale Crochet,[a] Victorio Cadierno,*[a] M. Isabel Menéndez[b] and Ramón López*[b]

The synthesis of a large variety of ureas $R^1R^2NC(=O)NH_2$ (R^1 and R^2 = alkyl, aryl or H; 26 examples) was successfully accomplished by hydration of the corresponding cyanamides $R^1R^2NC{\equiv}N$ using the phosphinous acid-based complexes $[MCl_2(\eta^6\text{-}p\text{-cymene})(PMe_2OH)]$ (M = Ru (**1**), Os (**2**)) as catalysts. The reactions proceeded cleanly under mild conditions (40-70 °C), in the absence of any additive, employing low metal loadings (1 mol%) and water as the sole solvent. In almost all the cases, the osmium complex **2** featured a superior reactivity in comparison to that of its ruthenium counterpart **1**. In addition, for both catalysts, the reaction rates observed for the hydration of the cyanamide substrates were remarkably faster than those involving classical aliphatic and aromatic nitriles. Computational studies allowed us to rationalize all these trends. Thus, the calculations indicated that the presence of a nitrogen atom directly linked to the C≡N bond depopulates electronically the nitrile carbon by inductive effect when coordinated to the metal center, thus favouring the intramolecular nucleophilic attack of the OH group of the phosphinous acid ligand to this carbon. On the other hand, the higher reactivity of Os *vs* Ru seems to be related with the lower ring strain on the incipient metallacycle that starts to form in the transition state associated with this key step in the catalytic cycle. Indirect experimental evidences of the generation of the metallacyclic intermediates were obtained by studying the reactivity of $[RuCl_2(\eta^6\text{-}p\text{-cymene})(PMe_2OH)]$ (**1**) towards dimethylcyanamide in methanol and ethanol. The reactions afforded compounds $[RuCl(\eta^6\text{-}p\text{-cymene})(PMe_2OR)(N{\equiv}CNMe_2)][SbF_6]$ (R = Me (**5a**), Et (**5b**)), resulting from the alcoholysis of the metallacycle, which could be characterized by single-crystal X-ray diffraction.

Introduction

Urea is an important structural motif in organic chemistry, present in a wide range of natural products, pharmaceuticals and agrochemicals.[1] The unique hydrogen binding capabilities of ureas make them also useful molecules for application in molecular recognition,[2] organocatalysis[3] or as gelators.[4] According to their relevance, a plethora of synthetic approaches can be found in the literature, the most common ones involving the reaction between phosgene (or more environmentally friendly surrogates like carbonate and carbamate derivatives) and amines, or the metal-catalyzed carbonylation of amines using CO or CO_2 as the source of the carbonyl unit.[5] Hofmann, Lossen and Curtius rearrangements are also well-known protocols to obtain urea derivatives, but, unfortunately, a number of drawbacks are encountered in all these classical routes, including a narrow substrate scope in some cases, the use of toxic and/or expensive reagents, harsh reaction conditions or multistep sequences. Thus, the search of expeditious and versatile protocols for the synthesis of ureas still remains a challenge for synthetic chemists. In this regard, the hydration of readily available cyanamides offers a simple and atom-economical entry to substituted ureas (Scheme 1).[6,7]

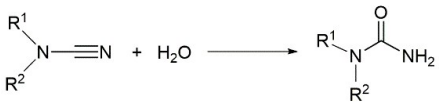

Scheme 1 The hydration of cyanamides to substituted ureas.

However, compared to the case of classical organonitriles R-C≡N (R = alkyl or aryl group), efforts devoted to develop efficient catalytic systems able to promote the hydration of cyanamides have been very scarce to date.[8] In fact, most of the examples quoted in the literature involve the use of strong Brønsted acids and bases as promoters, methods that suffer from drastic conditions, poor functional group compatibility and selectivity problems associated to the hydrolytic cleavage of the desired ureas, which leads to the formation of amines as by-products.[6,9] In the most recent years, the hydration of cyanamides to ureas have been selectively achieved, under remarkably mild conditions, employing TiO_2,[10a] Ag and Pd

[a] Laboratorio de Compuestos Organometálicos y Catálisis (Unidad Asociada al CSIC), Centro de Innovación en Química Avanzada (ORFEO-CINQA), Departamento de Química Orgánica e Inorgánica, Instituto Universitario de Química Organometálica "Enrique Moles", Facultad de Química, Universidad de Oviedo, Julián Clavería 8, E-33006 Oviedo, Spain. E-mail: vcm@uniovi.es
[b] Departamento de Química Física y Analítica, Universidad de Oviedo, Julián Clavería 8, E-33006 Oviedo, Spain. E-mail: rlopez@uniovi.es

Electronic Supplementary Information (ESI) available: Copies of the NMR spectra of the novel cyanamides **3h,l,r** and the ureas **4a-z** isolated from the catalytic reactions, and full details of the computational calculations. CCDC 1989797 (**5a**) and 1989798 (**5b**). For ESI and crystallographic data in CIF or other electronic format see DOI: 10.1039/x0xx00000x

nanoparticles,[10a-c] or Ag/bone nanocomposites.[10d] However, the scope of these heterogenous catalysts is restricted to *N*-aryl monosubstituted cyanamides.[11,12] Surprisingly, despite the fact that the addition of water to the C≡N bond of cyanamides is known to be favoured upon coordination to transition metals,[13] no homogeneous catalysts have been reported to date for the direct hydration of cyanamides. As a representative example, Bokach, Kukushkin and co-workers reported the synthesis of several *O*-bonded urea complexes $[ZnX_2\{O=C(NH_2)(NR_2)\}_2]$ (X= Cl, Br, I; R = aryl or alkyl group) upon heating compounds $[ZnX_2(N\equiv CNR_2)_2]$ in wet solvents without the aid of acidic or basic reagents.[14]

For long time we have been interested, from both experimental and mechanistic points of view, on the metal-catalyzed hydration of nitriles.[15] Among the different catalytic systems explored, the phosphinous acid-based ruthenium(II) and osmium(II) complexes $[MCl_2(\eta^6\text{-}p\text{-cymene})(PMe_2OH)]$ (M = Ru (**1**), Os (**2**); see Fig. 1) proved to be particularly effective, allowing to perform the hydration of a wide range of organonitriles in pure water, in the absence of any acidic or basic additive, with low metal loadings (1 mol%) and under relatively mild thermal conditions (80 °C).[16,17]

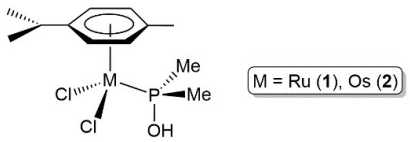

Fig. 1 Structure of half-sandwich Ru(II) and Os(II) complexes **1** and **2**.

Density functional theory (DFT) calculations on these systems also demonstrated the key role played by the Me_2POH ligand on the hydration process.[16] Thus, according to our calculations, the reactions proceed through the initial formation of a five-membered metallacyclic intermediate generated by intramolecular addition of the P-OH group of the phosphinous acid ligand to the metal-coordinated nitrile, with the subsequent hydrolysis of the metallacycle leading to the final amide product (Scheme 2).[18,19]

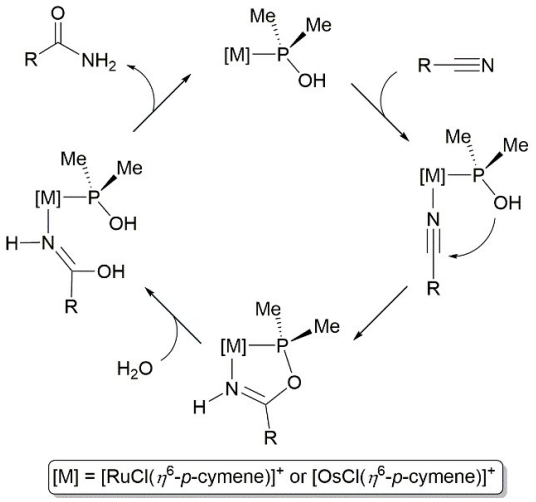

Scheme 2 Reaction pathway for the hydration of nitriles catalyzed by complexes **1** and **2**.

In this context, it is worthy to mention that Pregosin and co-workers were able to isolate the related metallacyclic compound **B** by reacting the arene-ruthenium(II) complex **A** with an excess of 4-methylbenzonitrile (Scheme 3).[20a] The X-ray crystal structure of **B** was subsequently reported by us along with its reactivity towards water, which led to the formation of the aquo-complex **C** with liberation of 4-methylbenzamide (see Scheme 3).[20b] Also of note is the fact that compound **B** is catalytically active in the hydration of 4-methylbenzonitrile into 4-methylbenzamide.[20b]

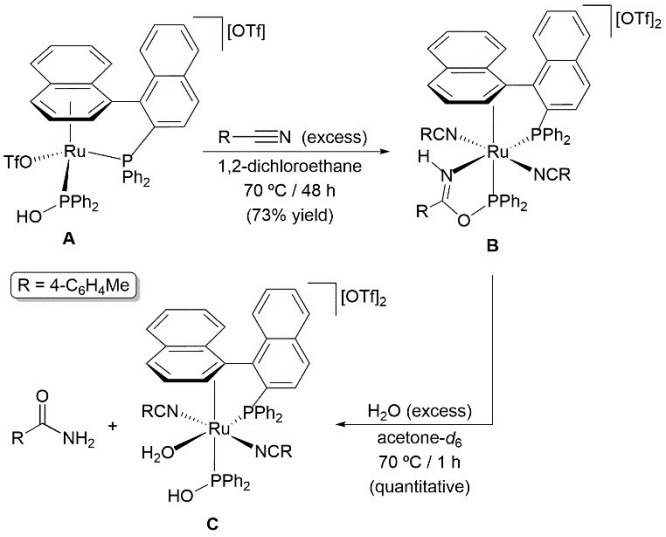

Scheme 3 Synthesis and hydrolytic cleavage of the ruthenacycle **B**.

With all these precedents in mind, and with the aim of discovering an efficient and general homogeneous system for the cyanamide-to-urea conversion, we decided to explore the catalytic potential of complexes $[MCl_2(\eta^6\text{-}p\text{-cymene})(PMe_2OH)]$ (M = Ru (**1**), Os (**2**)) for the selective hydration of cyanamides. The experimental results obtained are herein presented, along with additional theoretical investigations aimed to understand the different reaction rates observed between cyanamides and classical organonitriles.

Results and discussion

Catalytic hydration of cyanamides by the phosphinous acid-based Ru(II) and Os(II) complexes $[MCl_2(\eta^6\text{-}p\text{-cymene})(PMe_2OH)]$ (M = Ru (1), Os (2)).

The ability of complexes **1-2** to promote the hydration of cyanamides was first investigated employing commercially available dimethylcyanamide **3a** as a model substrate (see Table 1). Initial experiments were performed by adding the corresponding catalyst (1 mol%) to a 0.33 M aqueous solution of **3a**, and subsequent heating of the mixture in an oil bath at 80 °C. To our delight, a first control by gas chromatography (GC) at 15 minutes showed, for both reactions, the complete consumption of the starting cyanamide **3a** and the selective formation of the desired *N,N*-dimethylurea product **4a** (entries 1-2). Fast transformations were also observed when the same

View Article Online
DOI: 10.1039/D0CY00523A

reactions were performed at 40 °C (entries 3-4), and even at room temperature (entries 5-6). In addition, these experiments showed the greater effectiveness of the osmium complex **2** *vs* its ruthenium counterpart **1**, which allowed the quantitative formation of the urea **4a** after only 30 min (entry 4) or 1 h (entry 6).

Table 1 Catalytic hydration of dimethylcyanamide **3a** using complexes [$MCl_2(\eta^6$-*p*-cymene)(PMe_2OH)] (M = Ru (**1**), Os (**2**)).[a]

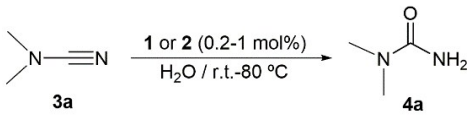

Entry	Catalyst	Loading	Temp. (°C)	*t* (h)	Yield (%)[b]
1	**1**	1 mol%	80	0.25	> 99
2	**2**	1 mol%	80	0.25	> 99
3	**1**	1 mol%	40	1	97
4	**2**	1 mol%	40	0.5	> 99
5	**1**	1 mol%	r.t.	4.5	97
6	**2**	1 mol%	r.t.	1	> 99
7	**2**	0.5 mol%	r.t.	1.5	> 99
8	**2**	0.2 mol%	r.t.	2	> 99
9[c]	**[Pt]**	1 mol%	80	1.5	3

[a] Reactions were performed under Ar atmosphere starting from 1 mmol of dimethylcyanamide (0.33 M in water). [b] Determined by GC (uncorrected GC areas). [c] Reaction performed with the Parkins platinum catalyst [$PtH\{(PMe_2O)_2H\}(PMe_2OH)$].

Reduction of the osmium loading to 0.5 or 0.2 mol% still produced **4a** in quantitative yield at r.t. without a drastic increase in the reaction time (1.5 and 2 h, respectively; entries 7 and 8), further demonstrating the remarkable reactivity of complex [$OsCl_2(\eta^6$-*p*-cymene)(PMe_2OH)] (**2**) (TOF and TON values up to 250 h^{-1} and 500, respectively). For comparative purposes, the conversion of **3a** into **4a** was also attempted with the Parkins complex [$PtH\{(PMe_2O)_2H\}(PMe_2OH)$] (1 mol%), which is probably the most versatile catalyst currently known for the hydration of nitriles.[8g,18] As shown in entry 9, the effectiveness of this catalyst was nearly null, leading only to trace amounts of **4a** after 1.5 h of heating at 80 °C (**3a** was recovered almost unchanged at the end of the process).

Table 2 Catalytic hydration of acetonitrile and benzonitrile using complexes [$MCl_2(\eta^6$-*p*-cymene)(PMe_2OH)] (M = Ru (**1**), Os (**2**)).[a]

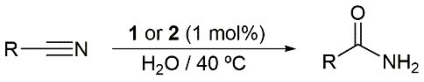

Entry	Nitrile	Catalyst	*t* (h)	Yield (%)[b]
1	R = Me	**1**	24	72
2	R = Me	**2**	24 (17)	> 99 (80)
3	R = Ph	**1**	5 (4)	> 99 (95)
4	R = Ph	**2**	24	80

[a] Reactions were performed under Ar atmosphere starting from 1 mmol of the corresponding nitrile (0.33 M in water). [b] Determined by GC (uncorrected GC areas).

Another aspect worth to be remarked is the fact that the reactivities shown by complexes **1** and **2** towards dimethylcyanamide **3a** are far superior to those found with classical organonitriles (aliphatic or aromatic).[16] Proof of that are the results collected in Table 2, showing the hydration of acetonitrile and benzonitrile with 1 mol% of **1** and **2** at 40 °C (to be compared with entries 3-4 in Table 1). Apparently, the presence of a N atom directly linked to the C≡N unit seems to favour the hydration process.

On the other hand, in order to determine the scope of complexes [$MCl_2(\eta^6$-*p*-cymene)(PMe_2OH)] (M = Ru (**1**), Os (**2**)), the hydration of a library comprising diverse cyanamide derivatives was next explored (see Table 3). The reactions were routinely performed at 40 °C with metal loadings of 1 mol%. Thus, as observed for **3a** (entry 1), other symmetrically (**3b-f**) and non-symmetrically (**3g-i**) disubstituted cyanamides could be cleanly converted into the corresponding *N,N*-disubstituted ureas **4b-i** (entries 2-9), with the osmium complex **2** showing in almost all the cases the best performance (GC yields ≥ 98% after 0.5-5.5 h). High conversions were also achieved employing **1** as catalyst, but at the expense of longer reaction times (except in the case of *N*-ethyl-*N*-phenylcyanamide **3g**; see entry 7). A very fast hydration of the parent cyanamide **3j** was observed with both catalysts, leading to urea **4j** in ≥ 96% GC-yield after only 15 min (entry 10). Further evidences of the generality of the process were gained employing different *N*-monosubstituted substrates (entries 11-26). The results obtained were clearly dependent on the aliphatic (**3k-r**) or aromatic (**3s-z**) nature of the substituent. Thus, for the former (entries 11-18), the best results were always obtained with the osmium catalyst **2** and, except in the case of the bulky cyanamide **3o** (entry 15), the reactions could be conveniently performed at 40 °C. On the contrary, for the aromatic substrates **3s-z** a remarkably longer reaction time (entry 19) or an increase of the temperature (70 °C; entries 20-26) was necessary to obtain the corresponding urea products **4s-z** in high yields. Moreover, a certain influence of the electronic nature of the aromatic ring was observed, the activity of the ruthenium complex **1** surpassing that of **2** when electron-withdrawing halide substituents (**3x-z**) are present (entries 24-26 *vs* 20-23). All the urea products **4a-z** were isolated in analytically pure form (61-94%) after chromatographic workup of the reactions carried out with the osmium catalyst **2**, thus allowing to unambiguously confirm their identities by NMR spectroscopy (see details in the Experimental section). We would like to emphasize at this point that, in none of the catalytic reactions studied in this work, the formation of amines as by-products was detected by GC in the crudes.

Mechanistic insights by computational chemistry calculations

We wanted to theoretically rationalize the differences in reactivity found between cyanamide and classical organonitrile hydrations (Table 2 *vs* 3). According to the thermodynamic formulation of the transition state theory (TF-TST),[21] the reaction rate depends exponentially on the Gibbs energy barrier, which causes that large differences in reaction times correspond to only small ones in Gibbs energy barriers. This is particularly important when comparing activation energy

Table 3 Catalytic hydration of cyanamides using complexes [$MCl_2(\eta^6$-*p*-cymene)(PMe_2OH)] (M = Ru (**1**), Os (**2**)): Scope of the process.[a]

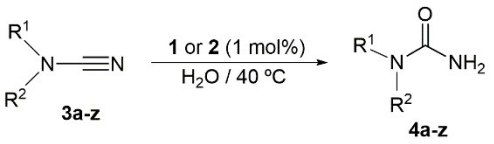

Entry	Substrate R^1/R^2	Catalyst	*t* (h)	Yield (%)[b]
1	Me/Me (**3a**)	**1**	1.5	**4a**; > 99
		2	0.5	**4a**; > 99 (92)
2	Et/Et (**3b**)	**1**	6.5	**4b**; 99
		2	2	**4b**; > 99 (91)
3	Bn/Bn (**3c**)	**1**	24	**4c**; 60
		2	5.5	**4c**; > 99 (80)
4	-$(CH_2)_4$- (**3d**)	**1**	1.5	**4d**; 96
		2	1.5	**4d**; > 99 (75)
5	-$(CH_2)_5$- (**3e**)	**1**	3	**4e**; > 99
		2	1.5	**4e**; > 99 (91)
6	-$(CH_2)_2O(CH_2)_2$- (**3f**)	**1**	1	**4f**; > 99
		2	0.5	**4f**; > 99 (94)
7	Et/Ph (**3g**)	**1**	0.5	**4g**; > 99
		2	1	**4g**; > 99 (89)
8	Et/$CH_2C(Me)=CH_2$ (**3h**)	**1**	1.5	**4h**; > 99
		2	1.5	**4h**; > 99 (83)
9	Cy/$CH_2CH=CH_2$ (**3i**)	**1**	7	**4i**; 96
		2	3	**4i**; 98 (62)
10	H/H (**3j**)	**1**	0.25	**4j**; 96
		2	0.25	**4j**; > 99 (80)
11	H/^{n}Pr (**3k**)	**1**	1	**4k**; > 99
		2	0.5	**4k**; > 99 (80)
12	H/^{i}Pr (**3l**)	**1**	2	**4l**; > 99
		2	0.5	**4l**; > 99 (82)
13	H/Cy (**3m**)	**1**	2	**4m**; > 99
		2	1	**4m**; > 99 (80)
14	H/^{t}Bu (**3n**)	**1**	7	**4n**; > 99
		2	1.5	**4n**; > 99 (75)
15[c]	H/1-Adamantyl (**3o**)	**1**	1.5	**4o**; 96
		2	1	**4o**; 96 (76)
16	H/Bn (**3p**)	**1**	6	**4p**; 84
		2	0.5	**4p**; > 99 (74)
17	H/(*S*)-CHMePh (**3q**)	**1**	7	**4q**; 91
		2	0.5	**4q**; > 99 (94)
18	H/(*R*)-CHMe-4-C_6H_4OMe (**3r**)	**1**	9	**4r**; 97
		2	1	**4r**; > 99 (86)
19	H/Ph (**3s**)	**1**	24	**4s**; 75
		2	24	**4s**; > 99 (68)
20[d]	H/2-C_6H_4Me (**3t**)	**1**	6.5	**4t**; 94
		2	3	**4t**; > 99 (82)
21[d]	H/3-C_6H_4Me (**3u**)	**1**	8	**4u**; 95
		2	1	**4u**; > 99 (72)
22[d]	H/4-C_6H_4Me (**3v**)	**1**	3.5	**4v**; > 99
		2	1.5	**4v**; > 99 (93)
23[d]	H/4-C_6H_4OMe (**3w**)	**1**	9.5	**4w**; 95
		2	5	**4w**; 95 (61)
24[d]	H/2-C_6H_4Cl (**3x**)	**1**	4	**4x**; > 99
		2	6.5	**4x**; 99 (70)
25[d]	H/4-C_6H_4Cl (**3y**)	**1**	3	**4y**; 93
		2	9	**4y**; 92 (63)
26[d]	H/2-C_6H_4Br (**3z**)	**1**	4	**4z**; > 99
		2	6.5	**4z**; > 99 (80)

[a] Reactions were performed under Ar atmosphere starting from 1 mmol of the corresponding cyanamide (0.33 M in water). [b] Determined by GC (uncorrected GC areas); isolated yields after work-up are given in brackets. [c] Reactions performed at 80 °C with a metal loading of 3 mol%. [d] Reactions performed at 70 °C.

barriers obtained from theoretical calculations aiming at reproducing and rationalizing experimental kinetic trends.[15b] For instance, the replacement of acetonitrile by dibenzylcyanamide reduces the time of their **1**-catalyzed hydration from 24 h to 5.5 h at 40 °C. Using TF-TST,[21] this implies a difference in Gibbs energy barriers of less than 1 kcal/mol at 40 °C, which is the chemical accuracy in computational chemistry.[22] This fact forces two requirements. On the one hand, a very accurate theoretical method should be used to calculate energy barriers. Thus, we used CPCM-DLPNO-CCSD(T)/def2-TZVPP//PCM-B3LYP/6-31+G(d,p) (LANL2DZ for Ru and Os) level of theory (see Computational Details section below and its justification in the ESI). For the sake of brevity, unless otherwise indicated, these computations will be henceforth denoted as DLPNO-CCSD(T). On the other hand, hydration processes with the largest possible difference in reaction times should be selected for comparison. Thus, we focused on the hydration of the cyanamide with the lowest reaction time (~ 0.25 h), *i.e.* **3j**, catalyzed by **1** and **2** (entry 10 in Table 3), to contrast with the hydration of classical organonitriles.

As for the hydration of acetonitrile and benzonitrile previously studied in our laboratory,[16] on the basis of the nature of the catalysts **1** and **2** and the cyanamide substrates considered herein, the most plausible reaction mechanisms for the hydration of **3j** are also the so-called intra- and intermolecular ones.[16a] The intramolecular mechanism proceeds through the nucleophilic attack by the hydroxyl group of the PMe_2OH ligand on the nitrile carbon atom of the metal-bonded cyanamide to form a metallacyclic intermediate (see for instance Scheme 2). This species undergoes the cleavage of the P-O bond by attack of a solvent water molecule on the P atom, thus leading to the generation and posterior release of the corresponding urea fragment. By analogy with the lower energy cost theoretically found for the amide elimination in closely related metal-catalyzed hydration of nitriles, the formation and hydrolytic opening of the metallacycle are the key mechanistic steps.[15b,c,16] Figs. 2 and S59 collect the optimized geometries of the species involved in those steps for the hydration of cyanamide **3j** catalyzed by **1** and **2**, whereas their energy data and Cartesian coordinates are reported in Tables S1-S3. To better follow the theoretical results, labels **1-OH-S_M**, **TS1-OH-S_M**, **2-OH-S_M**, and **TS2-OH-S_M** (**S** (substrate) = cyanamide (**cyan**), acetonitrile (**actn**), benzonitrile (**bzn**); **M** = Ru, Os) are used to identify the starting complex, the transition state (TS) for the hydroxyl attack, the metallacycle intermediate, and the TS for its cleavage, respectively. For the hydration of **3j**, the barrier for the hydroxyl attack is closer to that for the metallacycle opening (see Table S2). The difference between the energies of the two barriers reduces by 2.4/2.1 kcal/mol (acetonitrile → cyanamide) and 4.0/4.0 kcal/mol (benzonitrile → cyanamide) with **1**/**2**, respectively. In any case, for the cyanamide hydration, the Gibbs energy barrier of the nucleophilic attack step is still 3.3/2.4 kcal/mol (catalyst **1**/**2**) larger than the cleavage step. The highly sophisticated computational protocol here employed allows to confirm that the former step is the

View Article Online
DOI: 10.1039/D0CY00523A

rate-determining one (**1-OH-S_M** → **TS1-OH-S_M**). Once more the alternative intermolecular mechanism evolving through the PMe_2OH-assisted nucleophilic attack by one external solvent water molecule on the nitrile carbon atom does not compete with the one described above. For catalysts **1** and **2** the TS for such attack is 11.5 and 12.1 kcal/mol less stable than the analogous ones for the hydroxyl P-OH attack, **TS1-OH-cyan_Ru** and **TS1-OH-cyan_Os**, respectively (see **TS1-H_2O-cyan_Ru** and **TS1-H_2O-cyan_Os** in Fig. S60 and Tables S1-S3). Consequently, we focused on the formation step of the metallacycle intermediate of the intramolecular mechanism aiming at understanding the main experimental results achieved for cyanamide *vs* classical organonitrile hydration.

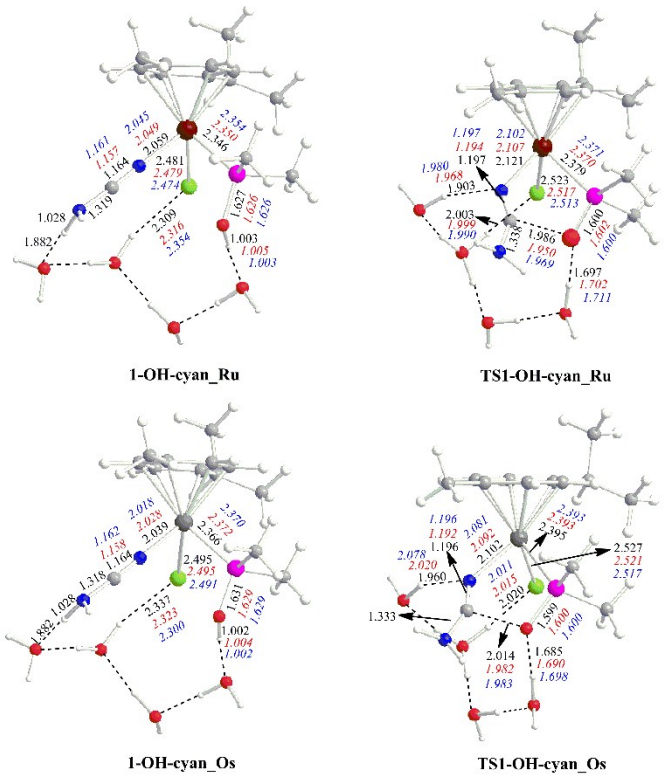

Fig. 2 Optimized geometries of the main species involved in the hydroxyl attack step of the cyanamide hydration reactions catalyzed by [$MCl_2(\eta^6$-*p*-cymene)(PMe_2OH)] (M = Ru (**1**), Os (**2**)). Distances are given in Å in black colour. For comparison purposes, analogous data for acetonitrile and benzonitrile hydration catalyzed by **1** and **2** are also included in red and blue colours, respectively.

As shown in Table 4 (first row), the replacement of acetonitrile (benzonitrile) by cyanamide diminishes the rate-determining Gibbs energy barrier by 3.6 kcal/mol (1.5 kcal/mol) when using the ruthenium catalyst **1**, while values of 1.5 kcal/mol (2.5 kcal/mol) were obtained in the case of the osmium catalyst **2**. This is in accordance with the experimental fact that hydration of **3j** is faster than that of acetonitrile and benzonitrile (compare reaction times for entry 10 in Table 3 to the corresponding ones in Table 2). Furthermore, the rate-determining Gibbs energy barrier obtained for the hydration of **3j** with **1** is 0.6 kcal/mol larger than the one with **2**, thus confirming the experimental evidences that the latter is, in general, more efficient for the hydration of cyanamide substrates than the former.

Table 4 DLPNO-CCSD(T) rate-determining Gibbs energy barrier, $\Delta G^{\ddagger}$, of the intramolecular mechanism investigated for the [$MCl_2(\eta^6$-*p*-cymene)(PMe_2OH)] (M = Ru (**1**), Os(**2**))-catalyzed hydration of the substrates (**S**) cyanamide, acetonitrile, and benzonitrile (**S** = **cyan**, **actn**, and **bzn**, respectively), electron delocalization index (DI) of the M-$N_{nitrile}$ and $C_{nitrile}$-$N_{nitrile}$ bonds at **1-OH-S_M** and of the $C_{nitrile}\cdots O_{hydroxyl}$ interaction at **TS1-OH-S_M**, area (A) of the metallacycle that is beginning to form at the rate-determining TS **TS1-OH-S_M** determined by M, P, $O_{hydroxyl}$, $C_{nitrile}$ and $N_{nitrile}$, and net natural atomic charge (NAC) of M, P, $O_{hydroxyl}$, $C_{nitrile}$, $N_{nitrile}$, and the atom directly linked to $C_{nitrile}$ (R) at **1-OH-S_M**.

	1 (Ru)			**2 (Os)**		
	cyan	**actn**	**bzn**	**cyan**	**actn**	**bzn**
$\Delta G^{\ddagger}$/kcal/mol	27.6	31.2	29.1	27.0	28.5	29.5
DI (M-$N_{nitrile}$)	0.6748	0.6921	0.7022	0.7596	0.7821	0.8033
DI ($C_{nitrile}$-$N_{nitrile}$)	1.9076	2.0311	2.0123	1.8787	1.9993	1.9771
DI ($C_{nitrile}\cdots O_{hydroxyl}$)	0.3255	0.3775	0.3689	0.3107	0.3590	0.3637
A/ Å^2	5.719	5.639	5.649	5.733	5.663	5.648
NAC(M)/*e*	0.15	0.14	0.15	0.27	0.27	0.27
NAC(P)/*e*	1.61	1.61	1.61	1.58	1.58	1.59
NAC($O_{hydroxyl}$)/*e*	-1.04	-1.04	-1.04	-1.05	-1.05	-1.04
NAC($C_{nitrile}$)/*e*	0.60	0.48	0.47	0.61	0.49	0.48
NAC($N_{nitrile}$)/*e*	-0.41	-0.34	-0.33	-0.43	-0.36	-0.35
NAC(R)/*e*	-0.89	-0.81	-0.21	-0.89	-0.81	-0.20

When comparing the most relevant distances of the optimized geometries obtained for **1-OH-S_M** and **TS1-OH-S_M** (see Fig. 2), it is noteworthy that the replacement of acetonitrile (benzonitrile) by cyanamide mainly changes the bond distance between the metal centre and the C≡N nitrogen atom ($N_{nitrile}$) at both **1-OH-S_M** and **TS1-OH-S_M**, and the distance between $O_{hydroxyl}$ and the attacked nitrile carbon atom ($C_{nitrile}$) at **TS1-OH-S_M**. Specifically, the Ru-$N_{nitrile}$ (Os-$N_{nitrile}$) bond length enlarges 0.010 (0.011) Å and 0.014 (0.021) Å when substituting acetonitrile and benzonitrile by cyanamide at **1-OH-S_M**, respectively. The same bond at **TS1-OH-S_M** lengthens 0.014 (0.010) Å and 0.019 (0.021) Å, respectively. Larger enlargements, 0.036 (0.032) Å and 0.027 (0.031) Å, were found for the $C_{nitrile}\cdots O_{hydroxyl}$ distance at **TS1-OH-S_M** when replacing acetonitrile and benzonitrile by cyanamide, respectively. Therefore, the presence of the metal-bonded cyanamide leads to the location of an earlier TS for the hydroxyl attack step and, consequently, to a lower rate-determining Gibbs energy barrier. In consonance with this, we have found that **TS1-OH-cyan_Os**, which presents the longest $C_{nitrile}\cdots O_{hydroxyl}$ distance (2.014 Å), determines the lowest rate-determining Gibbs energy barrier found (27.0 kcal/mol; see Table 4).

On the other hand, a topological analysis of the electron density within the framework of Bader's Atoms in Molecules (AIM) theory[23] allowed us to compute the electron delocalization indexes (DI)[24] between pairs of atoms at **1-OH-S_M** and **TS1-OH-S_M**. The DI is a measure of the number of electrons shared between two atoms and therefore, of the

covalency of the bond between them. According to our results in Table 4, the DI obtained for the Ru-$N_{nitrile}$ bond at **1-OH-S_Ru** diminishes from 0.6921 (**S** = **actn**) and 0.7022 (**S** = **bzn**) to 0.6748 (**S** = **cyan**), which is in good agreement for the enlargement found for such a bond distance. A similar diminution was found for **1-OH-S_Os** and **TS1-OH-S_M** (see Tables 4 and S4, respectively). Analogously, the DI of the $C_{nitrile}\cdots O_{hydroxyl}$ distances at **TS1-OH-S_M** follow the same trend. However, as the bond between $C_{nitrile}$ and $O_{hydroxyl}$ is not yet formed at the TS for the hydroxyl attack, DI($C_{nitrile}\cdots O_{hydroxyl}$) values are almost half of DI(M-$N_{nitrile}$) ones. It is also interesting to note that a reduction of the DI for the $C_{nitrile}$-$N_{nitrile}$ bond is also observed when the coordinated acetonitrile or benzonitrile molecules are replaced by cyanamide in both $[MCl(\eta^6\text{-}p\text{-cymene})(PMe_2OH)]^+$ fragments (see Table 4), despite a very small lengthening was found for the corresponding C≡N bond distances (less than 0.007 Å; see Fig. 2).

It is expected that the enlargement of the M-$N_{nitrile}$ and $C_{nitrile}\cdots O_{hydroxyl}$ distances at **TS1-OH-S_M** when cyanamide is present will lead to a more stable TS corresponding to a less strained metallacycle. Such a five-membered ring is determined by M (Ru or Os), P, $O_{hydroxyl}$, $C_{nitrile}$, and $N_{nitrile}$. As in our previous work on classical organonitriles hydration with **1** and **2**,[16b] we estimated the area of such an incipient metallacycle at **TS1-OH-cyan_M** and compared them with those found at **TS1-OH-actn_M** and **TS1-OH-bzn_M**. The area of the metallacycle was determined by adding the area of the triangle defined by the atoms M (Ru or Os), $N_{nitrile}$, and $C_{nitrile}$, plus that of the triangle of the atoms M, $C_{nitrile}$, and $O_{hydroxyl}$, plus that of the triangle of the atoms M, $O_{hydroxyl}$ and P (Fig. S61). We observed again that an important rise of this area reduces the magnitude of the Gibbs energy barrier. Specifically, the replacement of acetonitrile and benzonitrile by cyanamide enlarges the size of the metallacycle area from 5.639 and 5.649 $Å^2$ to 5.719 $Å^2$ with the ruthenium catalyst **1** (see Table 4). This rise is even greater for **2** and consequently the lowest rate-determining Gibbs energy barriers were obtained for cyanamide hydration catalyzed by the osmium complex **2** (27.0 kcal/mol), first, and then by **1** (27.6 kcal/mol).

In spite of all that, a question still needs to be solved, why are **TS1-OH-cyan_M** earlier TSs and therefore less strained than **TS1-OH-actn_M** and **TS1-OH-bzn_M**? A natural bond order (NBO) analysis[25] reflected no significant changes of the net atomic charge (NAC) for M, P and $O_{hydroxyl}$ when going from **1-OH-actn_M** and **1-OH-bzn_M** to **1-OH-cyan_M** (see Table 4). In contrast, the negative NAC of $N_{nitrile}$ at **1-OH-S_M** increases 0.07 and 0.08 *e* when replacing acetonitrile and benzonitrile by cyanamide, respectively, with both catalysts. An even greater variation, but in the opposite direction to the previous one, was observed for $C_{nitrile}$. Specifically, this atom depopulates electronically when passing from **1-OH-actn_Ru/Os**, NAC($C_{nitrile}$) = 0.48/0.49 *e*, and **1-OH-bzn_Ru/Os**, NAC($C_{nitrile}$) = 0.47/0.48 *e*, to **1-OH-cyan_Ru/Os**, NAC($C_{nitrile}$) = 0.60/0.61 *e*. This can be associated to the higher electronegativity of N *vs* C, which causes the NH_2 substituent to reduce much more sharply the electron density on $C_{nitrile}$ by inductive effect. Therefore, the presence of cyanamide instead of a classical organonitrile at the Ru and Os complexes increases the withdrawing of electron density from $C_{nitrile}$, thus favouring the establishment of an earlier and less unstable TS. In addition, a larger incipient metallacycle at the TS for the nucleophilic attack, along with a very slightly more positive NAC of $C_{nitrile}$, could explain why the Os catalyst **2** is more effective than the Ru one **1** for cyanamide hydration.

Experimental evidence of the formation of the metallacyclic intermediates

To obtain some experimental evidences on the mechanism we also studied the stoichiometric reactivity of complexes **1-2** towards dimethylcyanamide **3a**. In this regard, all our efforts to isolate the key metallacyclic intermediates by reacting **1** and **2** with variable amounts of **3a** and the chloride abstractors $NaSbF_6$ or $AgSbF_6$ in anhydrous THF failed. However, we found an indirect proof of their formation by carrying out the same reactions in methanol or ethanol. Thus, as shown in Scheme 4, the treatment of the ruthenium complex **1** with an excess of **3a** (10 equiv.) in the presence of $NaSbF_6$ lead to the formation of the cationic phosphinite complexes **5a,b**, which could be isolated in pure form in 49-59% yield.

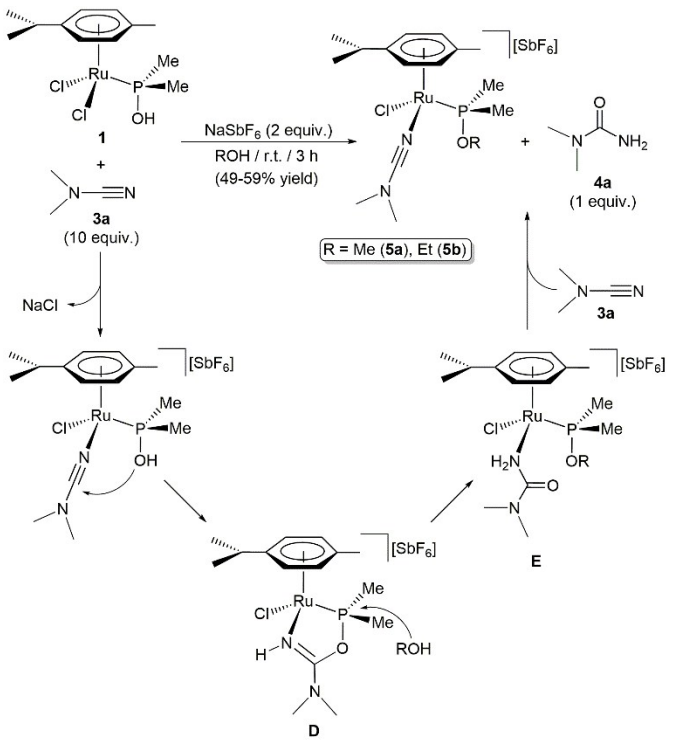

Scheme 4 Synthesis of the phosphinite-ruthenium(II) complexes **5a,b**.

The same reactivity was also observed with the osmium complex **2**, although in this case the reactions were not completely clean preventing the isolation of the corresponding products in pure form. Given that the OH/OR exchange on the *P*-donor ligand does not occur in the absence of **3a**, the formation of **5a,b** can only be explained through the initial generation of the metallacycle **D**, which evolves into the urea

complex **E** through alcoholysis with the solvent. Final displacement of the coordinated urea (**4a** was detected by NMR on the crudes) by a second molecule of **3a** leads to the isolated complexes **5a,b**.

To support the prevalence of the mechanism proposed in Scheme 4 we theoretically investigated, on the one hand, the formation of **D** and its transformation into **E** in methanol solution as they are the most energy-demanding steps of the intramolecular mechanism found for hydration of cyanamides and classical organonitriles in water solution. On the other hand, we also theoretically searched for a TS for the direct OH/OMe exchange in complex [RuCl(η^6-*p*-cymene)(PMe_2OH)(N≡$CNMe_2$)]$^+$ assisted by one external methanol molecule in methanol solution, but without the participation of the cyanamide. Fig. 3 collects the Gibbs energy profile obtained for the reactivity of complex **1** towards dimethylcyanamide (**dmcyan**) in methanol solution modelled by four explicit methanol molecules together with a polarizable continuum solvation medium characterized by the relative dielectric permittivity of the methanol solvent (ε = 32.6). More energy details and Cartesian coordinates of the species in Fig. 3 are shown in Tables S5-S7. As happened for the **1**-catalyzed cyanamide hydration in water solution, the formation step of the metallacyle **D** from complex [RuCl(η^6-*p*-cymene)(PMe_2OH)(N≡$CNMe_2$)]$^+$ (transformation **1-OH-dmcyan_Ru** → **TS1-OH-dmcyan_Ru** → **2-OH-dmcyan_Ru** in Fig. 3) is also once again more energy-demanding than the metallacycle cleavage step (transformation **2-OH-dmcyan_Ru** → **TS2-OH-dmcyan_Ru** → **3-OH-dmcyan_Ru** in Fig. 3). Specifically, according to our results, the formation of **D** (**2-OH-dmcyan_Ru** in Fig. 3) implies the surmounting of a Gibbs energy barrier of 29.5 kcal/mol, while a value of 25.3 kcal/mol is needed for the opening of the metallacycle in **D**. These energy barriers are only 1.9 and 1.0 kcal/mol larger than those found for the **1**-catalyzed hydration of cyanamide in water. Much more interestingly, the metallacycle **D** is a relatively very stable intermediate (-12.6 kcal/mol), 2.0 kcal/mol even more stable than the analogous one for the **1**-catalyzed hydration of cyanamide in water. Therefore, once **D** is formed, its evolution to **E**, $\Delta G^{\ddagger}$ = 25.3 kcal/mol, is much more favourable than going back to the complex [RuCl(η^6-*p*-cymene)(PMe_2OH)(N≡$CNMe_2$)]$^+$ (**1-OH-dmcyan_Ru** in Fig. 3), $\Delta G^{\ddagger}$ = 42.1 kcal/mol. In these circumstances, the precipitation of NaCl along with the formation of a very stable metallacyle intermediate seem to be the driving forces for the plausible formation of **5a** in light of the intramolecular mechanism assuming that the release of the urea moiety from **E** is not expected to compete with the remaining steps of the intramolecular mechanism.[15b,c,16] Alternatively, as commented above, we also explored the formation of **5a** via a direct OH/OMe exchange on the *P*-donor ligand at the [RuCl(η^6-*p*-cymene)(PMe_2OH)(N≡$CNMe_2$)]$^+$ complex (see Fig. S62 and Table S8). However, the Gibbs energy barrier obtained for such an exchange (57.0 kcal/mol) is much larger than the rate-determining one of the intramolecular mechanism, thus indicating that this route is not competitive with that passing through the formation of the metallacycle.

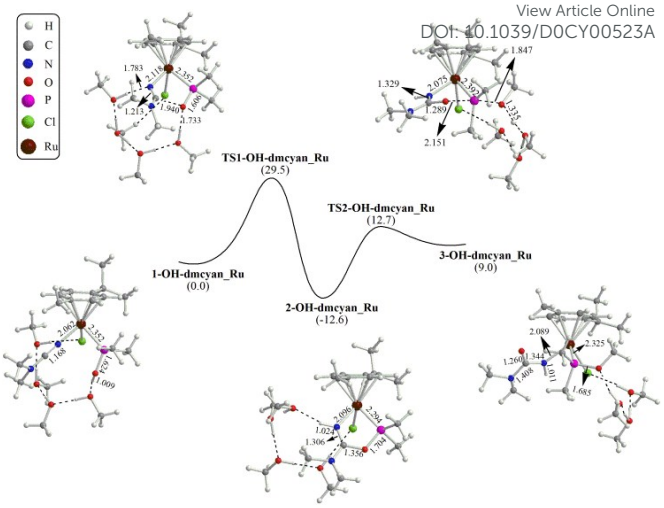

Fig. 3 DLPNO-CCSD(T) Gibbs energy profile obtained for the reactivity of complex **1** towards dimethylcyanamide (**dmcyan**) in methanol solution according to the intramolecular mechanism.

Compounds **5a,b** were fully characterized by means of elemental analysis and IR and multinuclear NMR spectroscopy, the data obtained being in complete agreement with the proposed formulations (details are given in the Experimental section). In particular, the transformation of the starting Me_2POH ligand into the corresponding phosphinite Me_2POR was evidenced in the ^{1}H and $^{13}C\{^1H\}$ NMR spectra by the appearance of characteristic signals for the OMe [δ_H = 3.73 ppm (d, $^3J_{PH}$ = 11.6 Hz); δ_C = 50.4 ppm (d, $^2J_{CP}$ = 10.1 Hz)] and OEt groups [δ_H = 1.43 (t, $^3J_{HH}$ = 6.9 Hz, CH_3) and 3.95-4.06 (m, CH_2); δ_C = 16.5 (d, $^3J_{CP}$ = 7.1 Hz, CH_3) and 63.4 ppm (d, $^2J_{CP}$ = 10.5 Hz, CH_2)]. In the spectra, the resonances associated to the C≡N (*ca.* δ_C = 124 ppm) and NMe_2 (δ_H = 3.00 ppm and δ_C = 40.1 ppm) groups of the coordinated dimethylcyanamide molecule could also be clearly identified.

In addition, single crystals suitable for X-ray diffraction analysis were obtained by slow diffusion of *n*-hexane into saturated solutions of the complexes in tetrahydrofuran, thus allowing to unequivocally confirm the structures proposed for **5a,b**. ORTEP-type views of the ruthenium cations are shown in Fig. 4 and selected bonding parameters collected in Table 5.

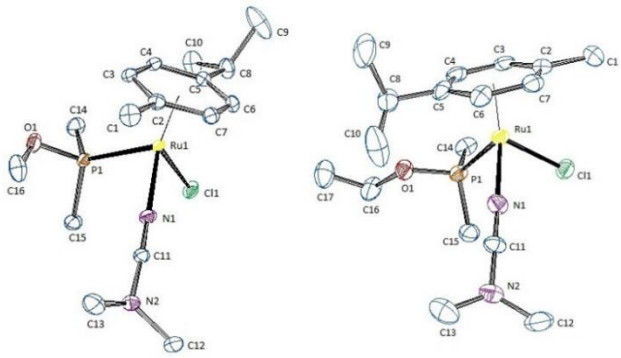

Fig. 4 ORTEP views of the structures of complexes **5a** (left) and **5b** (right) showing the crystallographic labelling scheme. Hydrogen atoms and SbF_6^- anions have been omitted for clarity. Thermal ellipsoids are drawn at 30% probability level.

Table 5 Selected bond distances (Å) and angles (°) for compounds **5a** and **5b**.[a]

	5a	5b
	Bond distances	
Ru-C*	1.7230(3)	1.7227(6)
Ru-Cl1	2.399(1)	2.400(2)
Ru-P1	2.305(1)	2.293(2)
Ru-N1	2.056(3)	2.060(7)
N1-C11	1.142(5)	1.14(1)
N2-C11	1.324(5)	1.31(1)
N2-C12	1.467(5)	1.45(1)
N2-C13	1.469(6)	1.46(1)
P1-O1	1.602(3)	1.600(6)
O1-C16	1.438(6)	1.431(1)
	Bond angles	
C*-Ru-P1	128.65(2)	128.36(5)
C*-Ru-Cl1	127.60(3)	128.18(6)
C*-Ru-N1	127.68(9)	128.8(2)
P1-Ru-Cl1	84.41(3)	83.11(7)
P1-Ru-N1	86.60(9)	86.4(2)
Cl1-Ru-N1	87.3(1)	86.7(2)
Ru-N1-C11	174.8(3)	173.8(7)
N1-C11-N2	176.2(4)	176.9(9)
C11-N2-C12	118.0(4)	117.4(8)
C11-N2-C13	116.6(4)	117.7(9)
C12-N2-C13	116.5(4)	117.1(9)
Ru-P1-O1	115.0(1)	108.5(2)
Ru-P1-C14	116.0(2)	113.6(3)
Ru-P1-C15	115.3(1)	117.6(3)

[a] C* denotes the centroid of the *p*-cymene ring (C2, C3, C4, C5, C6 and C7).

Both complexes exhibit the expected pseudo-octahedral three-legged piano-stool geometry, with the ruthenium atom bound to the *p*-cymene ring, one chloride anion, the phosphorus atom of the respective phosphinite ligand, and the C≡N nitrogen of one dimethylcyanamide molecule. The Ru-N1 bond lengths observed (2.056(3) and 2.060(7) Å) fit well to that described for $[RuCl_2(bpy)(CO)(N{\equiv}CNMe_2)]$ (2.043(3) Å), which is the only Ru(II) complex with a coordinated dimethylcyanamide ligand characterized by single-crystal X-ray diffraction reported to date in the literature.[26,27] The N1-C11 (1.142(5) and 1.14(1) Å) and C11-N2 (1.324(5) and 1.31(1) Å) distances, as well as the Ru-N1-C11 (174.8(3) and 173.8(7)°) and N1-C11-N2 (176.2(4) and 176.9(9)°) angles, are also very similar to those found in $[RuCl_2(bpy)(CO)(N{\equiv}CNMe_2)]$ (1.150(4) Å, 1.308(4) Å, 170.0(2)° and 178.3(3)°, respectively), the values observed suggesting a very small contribution of the bent resonance form **G** to the bonding of the dimethylcyanamide molecule (see Fig. 5).[28] On the other hand, the P-O bond distances of 1.602(3) and 1.600(6) Å found in the structures of **5a,b** are typical for phosphinite ligands coordinated to (η^6-*p*-cymene)-ruthenium(II) fragments.[29]

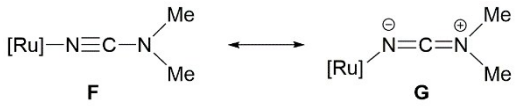

Fig. 5 Linear **F** and bent **G** resonance forms for the Ru-coordinated cyanamide molecule.

Conclusions

In summary, taking advantage of the ability of the phosphinous acid-based complexes $[MCl_2(\eta^6\text{-}p\text{-cymene})(PMe_2OH)]$ (M = Ru (**1**), Os (**2**)) to promote the catalytic hydration of nitriles under mild conditions, a highly efficient and selective protocol for the catalytic conversion of cyanamides to ureas has been developed. To the best of our knowledge, complexes **1-2** represent the first examples of homogeneous catalysts for this particular transformation reported in the literature. Remarkably, the reactivity of **1-2** toward cyanamides was found to be superior compared to that of classical organonitriles, with the osmium derivative **2** being in general more effective than its ruthenium counterpart **1**. According to our high-level computational studies (DLPNO-CCSD(T)), the higher reaction rates observed with the cyanamide substrates seems to be associated with the electronic depopulation that the NR_2 substituent induces on the nitrile carbon when coordinated to the metal centers. This favours the intramolecular nucleophilic attack of the OH group of the *P*-donor ligand to this carbon, which is the rate-limiting step in the catalytic cycle. On the other hand, the higher reactivity of Os *vs* Ru seems to be related with the lower ring strain on the incipient metallacycle that starts to form in the transition state associated with the just mentioned rate-limiting step.

Experimental

General methods

Synthetic procedures were performed under argon atmosphere using vacuum-line and standard Schlenk or sealed-tube techniques. Organic solvents were dried by standard methods and distilled under argon before use.[30] Complexes $[MCl_2(\eta^6\text{-}p\text{-cymene})(PMe_2OH)]$ (M = Ru (**1**),[17] Os (**2**)[16b]) were prepared following the method reported in the literature. The cyanamides employed in this work were obtained from commercial suppliers and used as received, or synthesized by reacting the corresponding amine with cyanogen bromide following the general protocol described by Kaushik and co-workers (details on the synthesis and characterization of the previously unreported compounds **3h,i,r** is given below).[31] NMR spectra were recorded at 25 °C on Bruker DPX-300 or AV400 instruments. $^{13}C\{^1H\}$ and ^1H NMR chemical shifts were referenced to the residual signal of deuterated solvent employed, and the $^{31}P\{^1H\}$ NMR ones to 85% H_3PO_4 as external standard. DEPT experiments have been carried out for all the compounds reported. Infrared spectra were recorded on a PerkinElmer 1720-XFT spectrometer. GC measurements were made on a Hewlett Packard HP6890 apparatus (Supelco Beta-Dex™ 120 column, 30 m length, 250 μm diameter). Elemental analyses were provided by the Analytical Service of the Instituto de Investigaciones Químicas (IIQ-CSIC) of Seville. HRMS data were obtained on a QTOF Bruker Impact II mass spectrometer in the General Services of the University of Oviedo. For column chromatography, Merck silica gel 60 (230-400 mesh) was employed.

Synthesis and characterization of cyanamides N≡CNR^{1}R^2 (R^1 = Et, R^2 = CH$_2$C(Me)=CH$_2$ (3h); R^1 = Cy, R^2 = CH$_2$CH=CH$_2$ (3i); R^1 = H, R^2 = (*R*)-CHMe-4-C$_6$H$_4$OMe (3r))

A solution of the corresponding amine (26 mmol) in 40 mL of diethyl ether was added dropwise to a stirred solution of cyanogen bromide (1.377 g, 13 mmol) in 80 mL of diethyl ether, previously cooled to 0 °C in an ice bath *(CAUTION: Cyanogen bromide is an extremely toxic chemical and should be used only in a well-ventilated fume hood while using the appropriate personal protective gear)*.[32] Once the addition finished, the reaction mixture was stirred at room temperature for 3 h and filtered. The filtrate was then washed with water (2 x 20 mL), dried with anhydrous $MgSO_4$, filtered and concentrated in vacuo to give a yellow oil, which was washed twice with hexane (2 x 10 mL). **(3h):** Yield: 1.162 g (72%). IR (film): ν = 2207 (s, C≡N) cm^{-1}. ^{1}H NMR ($CDCl_3$): δ = 5.00 and 4.98 (s, 1H each, =CH$_2$), 3.58 (s, 2H, NCH$_2$), 3.01 (q, 2H, $^3J_{HH}$ = 7.2 Hz, NC*H*$_2$CH$_3$), 1.80 (s, 3H, =CCH$_3$), 1.28 (t, 3H, $^3J_{HH}$ = 7.2 Hz, NCH$_2$C*H*$_3$) ppm. ^{13}C{^{1}H} NMR ($CDCl_3$): δ = 139.0 (s, =C), 117.8 (s, C≡N), 115.4 (s, =CH$_2$), 57.8 (s, NCH$_2$), 45.0 (s, NCH$_2$CH$_3$), 19.8 (s, =C*C*H$_3$), 12.7 (s, NCH$_2$*C*H$_3$) ppm. HRMS (ESI-TOF): *m/z* 125.108130 [M+H$^+$], $C_7H_{13}N_2$ requires 125.107325. **(3i):** Yield: 1.815 g (85%). IR (film): ν = 2203 (s, C≡N) cm^{-1}. ^{1}H NMR ($CDCl_3$): δ = 5.91-5.78 (m, 1H, =CH), 5.30 (d, 1H, $^3J_{HH}$ = 17.1 Hz, =CH$_2$), 5.28 (d, 1H, $^3J_{HH}$ = 10.2 Hz, =CH$_2$), 3.64 (d, 2H, $^3J_{HH}$ = 6.0 Hz, NCH$_2$), 2.77-2.69 (m, 1H, NCH), 1.97-1.12 (m, 10H, CH$_2$) ppm. ^{13}C{^{1}H} NMR ($CDCl_3$): δ = 131.9 (s, =C), 119.6 (s, =CH$_2$), 116.6 (s, C≡N), 58.4 (s, NCH), 52.8 (s, NCH$_2$), 30.9 (2C), 25.1 and 25.0 (2C) (s, CH$_2$) ppm. HRMS (ESI-TOF): *m/z* 187.121324 [M+Na$^+$], $C_{10}H_{16}N_2Na$ requires 187.120569. **(3r):** Yield: 2.016 g (88%). $[\alpha]_D^{20}$ = +173.0° (*c* 1.0, $CHCl_3$). IR (film): ν = 2214 (s, C≡N) cm^{-1}. ^{1}H NMR ($CDCl_3$): δ = 7.26 and 6.90 (d, 2H each, $^3J_{HH}$ = 8.7 Hz, CH$_{arom}$), 4.32-4.00 (m, 1H, NCH), 4.26 (br, 1H, NH), 3.80 (s, 3H, OMe), 1.53 (d, 3H, $^3J_{HH}$ = 6.6 Hz, Me) ppm. ^{13}C{^{1}H} NMR ($CDCl_3$): δ = 159.5 and 133.5 (s, C$_{arom}$), 127.5 and 114.2 (s, CH$_{arom}$), 115. 3 (s, C≡N), 55.3 (s, OMe), 55.0 (s, NCH), 21.9 (s, Me) ppm. HRMS (ESI-TOF): *m/z* 199.083351 [M+Na$^+$], $C_{10}H_{12}N_2ONa$ requires 199.084184.

General procedure for the catalytic hydration of cyanamides

Under argon atmosphere, the corresponding cyanamide **3a-z** (1 mmol), water (3 mL) and appropriate metallic complex **1** or **2** (0.01 mmol, 1 mol%; except for **3o** which required metal loadings of 3 mol%) were introduced into a Teflon-capped sealed tube, and the reaction mixture stirred at 40-80 °C for the indicated time (see Table 3). The course of the reaction was monitored by regularly taking samples of *ca.* 10 μL which, after extraction with CH_2Cl_2 (3 mL), were analysed by GC. For those reactions catalysed by the osmium(II) complex **2**, isolation of the urea products **4a-z** was performed as follows: Once the maximum conversion of the starting substrate was reached, the solvent was removed under vacuum and the resulting residue purified by flash column chromatography over silica gel, using EtOAc as eluent. The identity of the products was confirmed by ^{1}H and ^{13}C{^{1}H} NMR spectroscopy (copies of the NMR spectra have been included in the ESI file). Complete characterization data for the previously unreported ureas **4h,i,r** are as follows: **(4h):** Yellow solid. Yield: 0.118 g (83%). IR (KBr): ν = 3404 (br, N-H), 3226 (m, N-H), 1640 (s, C=O) cm^{-1}. ^{1}H NMR (CD_3OD): δ = 4.89 and 4.83 (s, 1H each, =CH$_2$), 3.83 (s, 2H, NCH$_2$), 3.27 (q, 2H, $^3J_{HH}$ = 7.2 Hz, NC*H*$_2$CH$_3$), 1.72 (s, 3H, =CCH$_3$), 1.37 (t, 3H, $^3J_{HH}$ = 7.2 Hz, NCH$_2$C*H*$_3$) ppm; NH$_2$ protons not observed. ^{13}C{^{1}H} NMR (CD_3OD): δ = 160.0 (s, C=O), 141.4 (s, =C), 110.2 (s, =CH$_2$), 51.4 (s, NCH$_2$), 41.0 (s, NCH$_2$CH$_3$), 19.6 (s, =C*C*H$_3$), 11.8 (s, NCH$_2$*C*H$_3$) ppm. HRMS (ESI-TOF): *m/z* 143.118826 [M+H$^+$], $C_{17}H_{15}N_2O$ requires 143.117890. **(4i):** Yellow oil. Yield: 0.113 g (62%). IR (film): ν = 3354 (br, N-H), 3208 (m, N-H), 1651 (s, C=O) cm^{-1}. ^{1}H NMR (CD_3OD): δ = 5.91-5.79 (m, 1H, =CH), 5.24-5.17 (m, 2H, =CH$_2$), 3.97 (br, 1H, NCH), 3.85-3.82 (m, 2H, NCH$_2$), 1.83-1.12 (m, 10H, CH$_2$) ppm; NH$_2$ protons not observed. ^{13}C{^{1}H} NMR (CD_3OD): δ = 160.0 (s, C=O), 135.6 (s, =C), 114.7 (s, =CH$_2$), 54.8 (s, NCH), 44.3 (s, NCH$_2$), 30.8 (2C), 25.6 (2C) and 25.1 (s, CH$_2$) ppm. HRMS (ESI-TOF): *m/z* 205.132173 [M+Na$^+$], $C_{10}H_{18}N_2NaO$ requires 205.131134. **(4r):** Yellow solid. Yield: 0.167 g (86%). $[\alpha]_D^{20}$ = +52.4° (*c* 1.0, CH_3OH). IR (KBr): ν = 3460 (br, N-H), 3287 (m, N-H), 1644 (s, C=O) cm^{-1}. ^{1}H NMR (CD_3OD): δ = 7.24 and 6.88 (d, 2H each, $^3J_{HH}$ = 8.7 Hz, CH$_{arom}$), 4.76 (q, 1H, $^3J_{HH}$ = 6.9 Hz, NCH), 3.78 (s, 3H, OMe), 1.40 (d, 3H, $^3J_{HH}$ = 6.9 Hz, Me) ppm; NH and NH$_2$ protons not observed. ^{13}C{^{1}H} NMR (CD_3OD): δ = 159.9 (s, C=O), 158.7 and 136.7 (s, C$_{arom}$), 126.6 and 113.4 (s, CH$_{arom}$), 54.3 (s, OMe), 48.7 (s, NCH), 22.0 (s, Me) ppm. HRMS (ESI-TOF): *m/z* 195.112208 [M+H$^+$], $C_{10}H_{15}N_2O_2$ requires 195.112804.

Synthesis and characterization of complexes [RuCl(η^6-*p*-cymene)(PMe$_2$OR)(N≡CNMe$_2$)][SbF$_6$] (R = Me (5a), Et (5b))

To a solution of complex [RuCl$_2$(η^6-*p*-cymene)(PMe$_2$OH)] (**1**) (0.038 g, 0.1 mmol) in 10 mL of the corresponding alcohol were added $NaSbF_6$ (0.052 g, 0.2 mmol) and dimethylcyanamide (80 μL, 1 mmol), and the resulting mixture stirred at room temperature for 3 h. The solvent was then removed under vacuum, the crude product extracted with CH_2Cl_2 (50 mL), and the extract filtered over Kieselguhr. Solvent removal and washing of the resulting residue with diethyl ether (3 x 10 mL) led to a yellow solid, which was dried in vacuo. **(5a):** Yield: 0.039 g (59%). IR (KBr): ν = 2281 (s, C≡N), 658 (s, SbF_6^-) cm^{-1}. ^{31}P{^{1}H} NMR (CD_2Cl_2): δ = 135.8 (s) ppm. ^{1}H NMR (CD_2Cl_2): δ = 5.79-5.73 (m, 3H, CH of cymene), 5.54 (d, 1H, $^3J_{HH}$ = 5.6 Hz, CH of cymene), 3.73 (d, 3H, $^3J_{PH}$ = 11.6 Hz, OMe), 3.00 (s, 6H, NMe$_2$), 2.69 (sept, 1H, $^3J_{HH}$ = 5.6 Hz, C*H*Me$_2$), 2.15 (s, 3H, Me), 1.94 (d, 3H, $^2J_{PH}$ = 9.6 Hz, PMe$_2$), 1.67 (d, 3H, $^2J_{PH}$ = 10.0 Hz, PMe$_2$), 1.29 and 1.27 (d, 3H each, $^3J_{HH}$ = 5.6 Hz, CH*Me*$_2$) ppm. ^{13}C{^{1}H} NMR ($CDCl_3$): δ = 123.9 (s, C≡N), 111.3 and 101.1 (s, C of cymene), 91.1 and 88.3 (s, CH of cymene), 89.7 (d, $^2J_{CP}$ = 4.6 Hz, CH of cymene), 88.7 (d, $^2J_{CP}$ = 3.2 Hz, CH of cymene), 54.0 (d, $^2J_{CP}$ = 10.1 Hz, OMe), 40.1 (s, NMe$_2$), 31.1 (s, *C*HMe$_2$), 22.1 and 22.0 (s, CH*Me*$_2$), 18.4 (s, Me), 18.1 (d, $^1J_{CP}$ = 35.6 Hz, P*Me*$_2$), 15.2 (d, $^1J_{CP}$ = 29.3 Hz, P*Me*$_2$) ppm. Elemental analysis calcd. (%) for $C_{16}H_{29}F_6N_2ClOPRuSb$: C 28.74, H 4.37, N 4.19; found: C 28.81, H 4.25, N 4.25. **(5b):** Yield: 0.033 g (49%). IR (KBr): ν = 2284 (s, C≡N), 658 (s, SbF_6^-) cm^{-1}. ^{31}P{^{1}H} NMR

(CD_2Cl_2): δ = 131.3 (s) ppm. ^{1}H NMR (CD_2Cl_2): δ = 5.78 (s, 2H, CH of cymene), 5.72 and 5.50 (d, 1H each, $^3J_{HH}$ = 5.7 Hz, CH of cymene), 4.06-3.95 (m, 2H, OCH_2), 3.00 (s, 6H, NMe_2), 2.70 (sept, 1H, $^3J_{HH}$ = 6.9 Hz, C*H*Me_2), 2.15 (s, 3H, Me), 1.95 and 1.68 (d, 3H each, $^2J_{PH}$ = 9.9 Hz, PMe_2), 1.43 (t, 3H, $^3J_{HH}$ = 6.9 Hz, OCH_2CH_3), 1.29 and 1.27 (d, 3H each, $^3J_{HH}$ = 6.9 Hz, CH*Me*$_2$) ppm. ^{13}C{^{1}H} NMR ($CDCl_3$): δ = 123.8 (s, C≡N), 111.0 and 101.6 (s, C of cymene), 90.9, 90.1, 88.7 and 87.9 (s, CH of cymene), 63.4 (d, $^2J_{CP}$ = 10.5 Hz, OCH_2), 40.1 (s, NMe_2), 31.1 (s, *C*HMe_2), 22.2 and 22.1 (s, CH*Me*$_2$), 18.4 (s, Me), 18.3 (d, $^1J_{CP}$ = 34.9 Hz, P*Me*$_2$), 16.5 (d, $^3J_{CP}$ = 7.1 Hz, OCH_2CH_3), 15.9 (d, $^1J_{CP}$ = 29.3 Hz, P*Me*$_2$) ppm. Elemental analysis calcd. (%) for $C_{17}H_{31}F_6N_2ClOPRuSb$: C 29.91, H 4.58, N 4.10; found: C 30.05, H 4.64, N 4.21.

X-ray crystal structure determination of compounds 5a and 5b

Crystals suitable for X-ray diffraction analysis were obtained in both cases by slow diffusion of *n*-hexane into a saturated solution of the complex in tetrahydrofuran. The most relevant crystal and refinement data are collected in Table 6. Data collection was performed with a Rigaku-Oxford Diffraction Xcalibur Onyx Nova single-crystal diffractometer using Cu-Kα radiation (λ = 1.5418 Å). Images were collected at a fixed crystal-to-detector distance of 62 mm using the oscillation method with 1.20° oscillation and 2.5-5.5 s variable exposure time per image for **5a**, and 1.00° oscillation and 11.0-40.0 s variable exposure time per image for **5b**. Data collection strategy was calculated with the program CrysAlis^{Pro} CCD.[33] Data reduction and cell refinement were performed with the program CrysAlis^{Pro} RED and an empirical absorption correction was applied using the SCALE3 ABSPACK algorithm as implemented in the program CrysAlis^{Pro} RED.[33]

The software package WINGX was used for space group determination, structure solution, and refinement.[34] The structures were solved by Patterson interpretation and phase expansion using SUPERFLIP.[35] Isotropic least-squares refinement on F^2 using SHELXL97 was performed.[36] During the final stages of the refinements, all the positional parameters and the anisotropic temperature factors of all non-H atoms were refined. For **5a**, the atoms F1 and F4 of the hexafluoroantimonate anion were found to be disordered over two alternative orientations. As suggested by SHELXL97, these disordered atoms were modelled with occupancy factor of 0.5639 for the major component and isotropically refined. For **5b**, three disordered atoms were found in the structure, *i.e.* the F2 atom of the SbF_6^- anion and the C9 and C10 carbons of the isopropyl unit of the *p*-cymene ligand. Although SHELXL97 provides two possible sites for each one, the anisotropic motion of the atoms on a single position leads to a better description of this positional disorder. All H atoms were geometrically located and their coordinates were refined riding on their parent atoms. The function minimized was $\{\Sigma[\omega(F_o^2 - F_c^2)^2]/\Sigma[\omega(F_o^2)^2]\}^{1/2}$ where $\omega = 1/[\sigma^2(F_o^2) + (aP)^2 + bP]$ (a and b values are collected in Table 6) with $\sigma(F_o^2)$ from counting statistics and P = [max (F_o^2, 0) +2F_c^2]/3. Atomic scattering factors were taken from International Tables for X-Ray Crystallography, Volume C.[37] Geometrical calculations related to the centroids C* were made with PARST.[38] The crystallographic plots were made with ORTEP.[34]

Table 6 Crystal data and structure refinement for compounds **5a** and **5b**.[a]

	5a	**5b**
Empirical formula	$C_{16}H_{29}F_6N_2ClOPRuSb$	$C_{17}H_{31}F_6N_2ClOPRuSb$
Formula weight	668.65	682.68
Temperature/K	150(2)	150(2)
Wavelength/Å	1.54184	1.54184
Crystal system	Monoclinic	Monoclinic
Space group	$P2_1/n$	$P2_1/n$
Crystal size/mm	0.04 x 0.12 x 0.28	0.03 x 0.15 x 0.25
a/Å	11.7394(1)	8.3717(3)
b/Å	14.7656(2)	21.5740(6)
c/Å	14.6955(2)	14.8558(6)
α (°)	90	90
β (°)	108.172(1)	105.025(4)
γ (°)	90	90
Z	4	4
Volume/Å^3	2420.26(5)	2591.39(16)
Calculated density/g cm^{-3}	1.835	1.750
μ/mm^{-1}	16.067	15.020
F(000)	1312	1344
ϑ range/°	4.23-69.59	3.70-69.81
Index ranges	$-14 \le h \le 11$	$-10 \le h \le 7$
	$-17 \le k \le 16$	$-15 \le k \le 26$
	$-17 \le l \le 17$	$-17 \le l \le 17$
Completeness to ϑ_{max}	98.4%	97.9%
Reflns. collected	12565	13035
Unique reflns.	4476 (R_{int} = 0.0370)	4791 (R_{int} = 0.0483)
Parameters/restraints	269/0	279/0
Refinement method	Full-matrix least-squares on F^2	
Goodness-of-fit on F^2	1.031	1.044
Weight function (a, b)	0.0414, 2.3912	0.0720, 16.1734
R_1 [$I > 2\sigma(I)$][a]	0.0323	0.0584
wR_2 [$I > 2\sigma(I)$][a]	0.0782	0.1477
R_1 (all data)	0.0370	0.0705
R_2 (all data)	0.0816	0.1647
Largest diff. peak and hole/e Å^{-3}	1.354, -0.895	2.278, -1.437

[a] $R_1 = \sum(||F_o|-|F_c||)/\sum|F_o|$; $wR_2 = \{\sum[w(F_o^2-F_c^2)^2]/\sum[w(F_o^2)^2]\}^{1/2}$

Computational chemistry details

As in previous theoretical investigations on metal-catalyzed hydration of nitriles,[16b] the most relevant species involved in the inter- and intramolecular mechanisms for the hydration of cyanamide catalyzed by [MCl_2(η^6-*p*-cymene)(PMe_2OH)] (M = Ru (**1**), Os (**2**)) were fully optimized in water solution from the outset at the PCM-B3LYP/6-31+G(d,p) (LANL2DZ for Ru and Os)[39-42] using a modified version of the Schlegel's algorithm.[43] The same computational level was also employed to optimize in methanol solvent the key species of the intramolecular mechanism proposed in Scheme 4 and the direct OH/OMe exchange in the [RuCl(η^6-*p*-cymene)(PMe_2OH)(N≡CNMe_2)]$^+$ complex for the reactivity of [$RuCl_2$(η^6-*p*-cymene)(PMe_2OH)] towards dimethylcyanamide in alcoholic media. The nature of the critical structures located was confirmed by means of analytical computations of harmonic vibrational frequencies. The connectivity between each transition state (TS) and the

corresponding stable species found was initially checked by the normal-mode analysis of the imaginary frequency in the TS as they are analogous to those found for the acetonitrile and benzonitrile hydration catalyzed by **1** and **2**.[16b] Nonetheless, taking into account that the attacking hydroxyl oxygen atom of the PMe_2OH ligand is quite distant (~ 3.5 Å) from the attacked C≡N carbon atom in the metallacycle formation step, we thoroughly explored the connectivities **1-OH-cyan_M** → **TS1-OH-cyan_M** → **2-OH-cyan_M** (**M** = **Ru**, **Os**) in water solution and **1-OH-dmcyan_Ru** → **TS1-OH-dmcyan_Ru** → **2-OH-dmcyan_Ru** in methanol solution by means of intrinsic reaction coordinate (IRC) computations with the second order Gonzalez-Schlegel integration method.[44] Figs. S63-S65 show the evolution of each TS towards the corresponding minima and confirm the connectivities mentioned above. Gibbs free energies in solution (G) were calculated through the ideal gas, rigid rotor, and harmonic oscillator approximations at a pressure of 1 atm and a temperature of 298.15 K, which are typically used for computing gas-phase thermodynamic properties.[45] This is a standard procedure that has proven to be a correct and useful approach.[46] All these computations were performed with the Gaussian 09 series of programs (G09).[47]

To get more accurate energies (particularly energy barriers), single-point energy calculations on the PCM-B3LYP/6-31G+(d,p) (LANL2DZ for Ru and Os) optimized geometries were performed using the domain localized pair natural orbital-coupled cluster approach with single, double, and perturbative triple excitations (DLPNO-CCSD(T)).[48] The balanced Karlsruhe triple-zeta basis set def2-TZVPP[49] and the conductor-like polarizable continuum model (CPCM)[50] were used in the DLPNO-CCSD(T) computations. All organometallic systems investigated showed T1 diagnostic values less than 0.02,[51] suggesting that a multi-reference treatment is not necessary. In general, DLPNO-CCSD(T) energies are more accurate than B3LYP ones using at least a triple-zeta quality basis set.[52] For comparison purposes, the PCM-B3LYP/6-31G+(d,p) (LANL2DZ for Ru and Os) energies of the species involved in the $[MCl_2(\eta^6\text{-arene})(PMe_2OH)]$ (M = Ru (**1**), Os (**2**))-catalyzed hydration of acetonitrile and benzonitrile were also refined at the CPCM-DLPNO-CCSD(T)/def2-TZVPP level (Tables S1 and S2 in the ESI). The RI (resolution of the identity) approximation[53] as implemented in the ORCA program version 4.0.1[54] was employed, using the def2/JK auxiliary basis set[49a,55] for the Coulomb and exchange integrals as well as the def2-TZVPP/C auxiliary basis set[56] for the RI-DLPNO-CCSD(T)-like part. These calculations employed the ORCA program[54] and the frozen-core approximation. More technical details on the computational chemistry tools mentioned above as well as a justification for the choice of the DLPNO-CCSD(T) method are included in the ESI file.

Finally, to shed light on the factors governing the kinetic trends experimentally detected and theoretically confirmed, we carried out different theoretical analyses on the B3LYP electron density of some of the relevant species. Electron delocalization indexes between two atoms *A* and *B* in a molecule, $\delta(A,B)$ = DI,[24] were computed using AIMAll program[57] within the framework of Bader's Atoms in Molecules (AIM) theory.[23] The natural bond orbital (NBO)[25] method was also used in some relevant species to obtain net natural atomic charges (NAC) as implemented in G09.

Conflicts of interest

There are no conflicts to declare.

Acknowledgements

Financial support from the Spanish Ministry of Economy, Industry and Competitiveness (MINECO projects CTQ2016-75986-P and PG2018-100013-B-I00) and the University of Oviedo (project PAPI-18-GR-2011-0032) is gratefully acknowledged. R.G.-F. thanks MECD of Spain for the award of a FPU fellowship.

Notes and references

1 See, for example: (*a*) H.-Q. Li, P.-C. Lv, T. Yan and H.-L. Zhu, *Anti-Cancer Agents Med. Chem*. 2009, **9**, 471; (*b*) N. Volz and J. Clayden, *Angew. Chem. Int. Ed.*, 2011, **50**, 12148; (*c*) E. Delebecq, J.-P. Pascault, B. Boutevin and F. Ganachaud, *Chem. Rev.*, 2013, **113**, 80; (*d*) P. Sikka, J. K. Sahu, A. K. Mishra and S. R. Hashim, *Med. Chem.*, 2015, **5**, 479; (*e*) L. Garuti, M. Roberti, G. Bottegoni and M. Ferraro, *Curr. Med. Chem.*, 2016, **23**, 1528; (*f*) A. D. Jagtap, N. B. Kondekar, A. A. Sadani and J.-W. Chen, *Curr. Med. Chem.*, 2017, **24**, 622.

2 (*a*) V. Amendola, L. Fabbrizzi and L. Mosca, *Chem. Soc. Rev.*, 2010, **39**, 3889; (*b*) P. Dydio, D. Lichosyt and J. Jurczak, *Chem. Soc. Rev.*, 2011, **40**, 2971; (*c*) R. Custelcean, *Chem. Commun.*, 2013, **49**, 2173; (*d*) V. B. Bregović, N. Basarić and K. Mlinarić-Majerski, *Coord. Chem. Rev.* 2015, **295**, 80; (*e*) D. Yang, J. Zhao, X.-J. Yang and B. Wu, *Org. Chem. Front.*, 2018, **5**, 662.

3 (*a*) X. Yu and W. Wang, *Chem. Asian J.*, 2008, **3**, 516; (*b*) A. G. Doyle and E. N. Jacobsen, *Chem. Rev.*, 2007, **107**, 5713; (*c*) Z. Zhang and P. R. Schreiner, *Chem. Soc. Rev.*, 2009, **38**, 1187; (*d*) M. Tsakos and C. G. Kokotos, *Tetrahedron*, 2013, **69**, 10199; (*e*) A. Franconetti and G. de Gonzalo, *ChemCatChem*, 2018, **10**, 5554; (*f*) B. Atashkar, M. A. Zolfigol and S. Mallakpour, *Mol. Catal.*, 2018, **452**, 192.

4 (*a*) J. W. Steed, *Chem. Soc. Rev.*, 2010, **39**, 3686; (*b*) M. Yamanaka, *J. Incl. Phenom. Macrocycl. Chem.*, 2013, **77**, 33; (*c*) Y. Ohsedo, *Polym. Adv. Technol.*, 2016, **27**, 704; (*d*) M. Yamanaka, *Polym. J.*, 2018, **50**, 627; (*e*) B. Maiti, A. Abramov, R. Pérez-Ruiz and D. D. Díaz, *Acc. Chem. Res.*, 2019, **52**, 1865.

5 For reviews covering synthetic approaches to urea derivatives, see: (*a*) D. F. Kutepov, *Russ. Chem. Rev.*, 1962, **31**, 633; (*b*) T. P. Vishnyakova, I. A. Golubeva and E. V. Glebova, *Russ. Chem. Rev.*, 1985, **54**, 249; (*c*) F. Bigi, R. Maggi and G. Sartori, *Green Chem.*, 2000, **2**, 140; (*d*) I. Gallou, *Org. Prep. Proced. Int.*, 2007, **39**, 355; (*e*) H. Wang, Z. Xin and Y. Li, *Top. Curr. Chem.*, 2017, **375**, 49; (*f*) V. Štrukil, *Belstein J. Org. Chem.*, 2017, **13**, 1828; (*g*) X. He, X.-Y. Li, Y. Song, S.-M. Xia, X.-D. Lang and L.-N. He, *Curr. Organocat.*, 2017, **4**, 112; (*h*) A. V. Smolobochkin, A. S. Gazizov, A. R. Burilov and M. A. Pudovic, *Russ. Chem. Bull.*, 2019, **68**, 662.

6 For reviews covering the chemistry of cyanamides, see: (*a*) D. D. Nekrasov, *Russ. J. Org. Chem.*, 2004, **40**, 1387; (*b*) M.-H. Larraufie, G. Maestri, M. Malacria, C. Ollivier, L. Fensterbank and E. Lacôte, *Synthesis*, 2012, **44**, 1279; (*c*) M. R. R. Prabhath, L. Williams, S. V. Bhat and P. Sharma, *Molecules*,

2017, **22**, 615; (*d*) J.-T. Yu, F. Teng and J. Cheng, *Adv. Synth. Catal.*, 2017, **359**, 26.

7 The reverse process, *i.e.* the dehydration of ureas, can also be employed for the preparation of cyanamides. However, the most prevalent methods for the synthesis of both mono- and disubstituted cyamanides are (*i*) the direct alkylation of sodium, potassium or calcium cyanamide and (*ii*) the electrophilic cyanation of primary or secondary amines. In addition, severe reaction conditions are usually required to achieve the dehydration of ureas (see ref. 6).

8 For reviews covering the catalytic hydration of nitriles, see: (*a*) V. Y. Kukushkin and A. J. L. Pombeiro, *Chem. Rev.*, 2002, **102**, 1771; (*b*) V. Y. Kukushkin and A. J. L. Pombeiro, *Inorg. Chim. Acta*, 2005, **358**, 1; (*c*) T. J. Ahmed, S. M. M. Knapp and D. R. Tyler, *Coord. Chem. Rev.*, 2011, **255**, 949; (*d*) R. García-Álvarez, P. Crochet and V. Cadierno, *Green Chem.*, 2013, **15**, 46; (*e*) R. García-Álvarez, J. Francos, E. Tomás-Mendivil, P. Crochet and V. Cadierno, *J. Organomet. Chem.*, 2014, **771**, 93; (*f*) E. L. Downs and D. R. Tyler, *Coord. Chem. Rev.*, 2014, **280**, 28; (*g*) V. Cadierno, *Appl. Sci.*, 2015, **5**, 380; (*h*) M. A. Hussain and J. W. Kim, *Appl. Chem. Eng.*, 2015, **26**, 128; (*i*) M.-X. Wang, *Acc. Chem. Res.*, 2015, **48**, 602; (*j*) K. Singh, A. Sarbaina and J. K. Bera, *J. Indian Chem. Soc.*, 2018, **95**, 853.

9 For illustrative examples, see: (*a*) E. B. Vliet, *J. Am. Chem. Soc.*, 1924, **46**, 1305; (*b*) T. Mukaiyama, S. Ohishi and H. Takamura, *Bull. Chem. Soc. Jpn.*, 1954, **27**, 416; (*c*) Y. L. Chow and K. E. Haque, *Can. J. Chem.*, 1968, **46**, 2901; (*d*) S. Nag, G. P. Yadav, P. R. Maulik and S. Batra, *Synthesis*, 2007, 911; (*e*) V. D. Jadhav, E. Herdtweck and F. P. Schmidtchen, *Chem. Eur. J.*, 2008, **14**, 6098.

10 (*a*) N. Nasrollahzadeh, *RSC Adv.*, 2014, **4**, 29089; (*b*) Z. Issaabadi, N. Nasrollahzadeh and S. M. Sajadi, *J. Colloid Interface Sci.*, 2017, **503**, 57; (*c*) D. Habibi, S. Heydari, A. Faraji, H. Keypour and M. Mahmoudabadi, *Polyhedron*, 2018, **151**, 520; (*d*) S. S. Momeni, N. Nasrollahzadeh, A. Rustaiyan, *J. Colloid Interface Sci.*, 2017, **499**, 93.

11 Alternative protocols for the hydration of cyanamides in organic media, employing acetaldoxime as a water surrogate and catalytic systems based on $InCl_3$, nano CeO_2 and CuO nanoparticles, have also appeared: (*a*) S. H. Kim, B. R. Park and J. N. Kim, *Bull. Korean Chem. Soc.*, 2011, **32**, 716; (*b*) S. M. Sajadi and M. Maham, *J. Chem. Res.*, 2013, **37**, 623; (*c*) N. Nasrollahzadeh, M. Maham and S. M. Sajadi, *J. Colloid Interface Sci.*, 2015, **455**, 245.

12 Contrary to the case of simple carbonitriles (see reference 8i), no general protocols for the enzymatic hydration of cyanamides are currently available. Only the conversion of unsubstituted cyanamide into urea catalyzed by some particular enzymes has been described: (*a*) U. H. Maier-Greiner, B. M. Obermaier-Skrobranek, L. M. Estermaier, W. Kammerloher, C. Freund, C. Wülfing, U. I. Burkert, D. H. Matern, M. Breuer and M. Eulitz, *Proc. Natl. Acad. Sci. U.S.A.*, 1991, **88**, 4260; (*b*) F. Briganti, S. Mangani, A. Scozzafava, G. Vernaglione and C. T. Supuran, *J. Biol. Inorg. Chem.*, 1999, **4**, 528; (*c*) A. Guerri, F. Briganti, A. Scozzafava, C. T. Supuran and S. Mangani, *Biochemistry*, 2000, **39**, 12391; (*d*) J. Li, M. Biss, Y. Fu, X. Xu, S. A. Moore and W. Xiao, *J. Biol. Chem.*, 2015, **290**, 12664.

13 (*a*) N. A. Bokach and V. Y. Kukushkin, *Coord. Chem. Rev.*, 2013, **257**, 2293 and references cited therein; (*b*) P. Tong, D. Yang, Y. Li, B. Wang and J. Qu, *Organometallics*, 2015, **34**, 3571.

14 A. S. Smirnov, E. S. Butukhanova, N. A. Bokach, G. L. Starova, V. V. Gurzhiy, M. L. Kuznetsov and V. Y. Kukushkin, *Dalton Trans.*, 2014, **43**, 15798.

15 See, for example: (*a*) V. Cadierno, J. Díez, J. Francos and J. Gimeno, *Chem. Eur. J.*, 2010, **16**, 9808; (*b*) E. Tílvez, M. I. Menéndez and R. López, *Organometallics*, 2012, **31**, 1618; (*c*) E. Tílvez, M. I. Menéndez and R. López, *Inorg. Chem.*, 2013, **52**, 7541; (*d*) R. García-Álvarez, M. Zablocka, P. Crochet, C. Duhayon, J.-P. Majoral and V. Cadierno, *Green Chem.*, 2013, **15**, 2447; (*e*) E. Tomás-Mendivil, R. García-Álvarez, C. Vidal, P. Crochet and V. Cadierno, *ACS Catal.*, 2014, **4**, 1901; (*f*) R. González-Fernández, P. J. González-Liste, J. Borge, P. Crochet and V. Cadierno, *Catal. Sci. Technol.*, 2016, **6**, 4398; (*g*) E. Tomás-Mendivil, J. Francos, R. González-Fernández, P. J. González-Liste, J. Borge and V. Cadierno, *Dalton Trans.*, 2016, **45**, 13590; (*h*) R. González-Fernández, P. Crochet and V. Cadierno, *Org. Lett.*, 2016, **18**, 6164.

16 (*a*) E. Tomás-Mendivil, V. Cadierno, M. I. Menéndez and R. López, *Chem. Eur. J.*, 2015, **21**, 16874; (*b*) R. González-Fernández, P. Crochet, V. Cadierno, M. I. Menéndez and R. López, *Chem. Eur. J.*, 2017, **23**, 15210.

17 The utility of complex $[RuCl_2(\eta^6\text{-}p\text{-cymene})(PMe_2OH)]$ (**1**) had been previously demonstrated by Tyler and co-workers: S. M. M. Knapp, T. J. Sherbow, R. B. Yelle, J. J. Juliette and D. R. Tyler, *Organometallics*, 2013, **32**, 3744.

18 A similar mechanism was also proposed for the well-known Parkins platinum catalyst $[PtH\{(PMe_2O)_2H\}(PMe_2OH)]$: (*a*) T. Ghaffar, A. W. Parkins, *Tetrahedron Lett.*, 1995, **36**, 8657; (*b*) *J. Mol. Catal. A: Chem.*, 2000, **160**, 249.

19 The non-innocent role of phosphinous acids R_2POH in other catalytic transformations, such as Ru-catalyzed C-H bond activation and C=C bond isomerization processes, has also been documented. See, for example: (*a*) A. Gallen, A. Riera, X. Verdaguer and A. Grabulosa, *Catal. Sci. Technol.*, 2019, **9**, 5504; (*b*) J. Francos, D. Elorriaga, P. Crochet and V. Cadierno, *Coord. Chem. Rev.*, 2019, **387**, 199; (*c*) R. González-Fernández, P. Crochet and V. Cadierno, *Organometallics*, 2019, **38**, 3696.

20 (*a*) T. J. Geldbach, D. Drago and P. S. Pregosin, *J. Organomet. Chem.*, 2002, **643-644**, 214; (*b*) E. Tomás-Mendivil, L. Menéndez-Rodríguez, J. Francos, P. Crochet and V. Cadierno, *RSC Adv.*, 2014, **4**, 63466.

21 (*a*) J. I. Steinfeld, J. S. Francisco and W. L. Hase, in *Chemical Kinetics and Dynamics*, 2nd Ed., Prentice Hall, New Jersey, 1999; (*b*) The inverse of the rate constant determined in accordance with the thermodynamic formulation of TST gives an estimate of how long a given reaction takes.

22 J. A. Pople, *Rev. Mod. Phys.*, 1999, **71**, 1267.

23 (*a*) R. F. W. Bader, in A*toms in Molecules. A Quantum Theory*, University Press: Oxford, 1990; (*b*) R. F. W. Bader, *Chem. Rev.*, 1991, **91**, 893; (*c*) R. F. W. Bader, P. L. A. Popelier and T. A. Keith, *Angew. Chem. Int. Ed.*, 1994, **33**, 620.

24 (*a*) X. Fradera, M. A. Austen, R. F. W. Bader, *J. Phys. Chem. A*, 1999, **103**, 304; (*b*) X. Fradera, J. Poater, S. Simon, M. Durán, M. Solá, *Theor. Chem. Acc.*, 2002, **108**, 214.

25 (*a*) F. Weinhold and C. R. Landis, in *Valency and Bonding: A Natural Bond Orbital Donor-Acceptor Perspective*, Cambridge University Press, Cambridge, 2005; (*b*) *NBO, Version 3.1*, E. D. Glendening, A. E. Reed, J. E. Carpenter and F. Weinhold, University of Wisconsin, Madison, WI, 2012.

26 N. A. Bokach, M. Haukka, P. Hirva, M. F. C. G. D. Silva, V. Y. Kukushkin and A. J. L. Pombeiro, *J. Organomet. Chem.*, 2006, **691**, 2368.

27 For examples involving other cyanamides, see: (*a*) G. Albertin, S. Antoniutti and J. Castro, *Eur. J. Inorg. Chem.*, 2009, 5352; (*b*) G. Albertin, S. Antoniutti, S. Caia and J. Castro, *Dalton Trans.*, 2014, **43**, 7314.

28 The computed species **1-OH-S_M** show M-$N_{nitrile}$-$C_{nitrile}$ and $N_{nitrile}$-$C_{nitrile}$-R bond angles very similar to those found in the X-ray crystal structures of **5a** and **5b**, as they range from 176.9 to 178.6° and from 176.6 to 179.4°, respectively. As nicely discussed in ref. 13*a*, a significant contribution of the bent resonance form in a metal-coordinated cyanamide should lead to M-$N_{nitrile}$-$C_{nitrile}$ angles < 170°. The negligible

contribution of such a resonance in the present systems seems to be consistent with the catalytic trends observed, since an increase of the electron density on the carbon atom would be expected in such a bonding situation (mesomeric effect), thus disfavouring the key nucleophilic attack of the P-OH unit.

29 See, for example: (*a*) P. Crochet, J. Díez, M. A. Fernández-Zúmel and J. Gimeno, *Adv. Synth. Catal.*, 2006, **348**, 93; (*b*) S. M. M. Knapp, L. N. Zakharov and D. R. Tyler, *Acta Cryst.*, 2012, **E68**, m1465; (*c*) R. Sun, X. Chu, S. Zhang, T. Li, Z. Wang and B. Zhu, *Eur. J. Inorg. Chem.*, 2017, 3174; (*d*) B. Choubey, P. S. Prasad, J. T. Mague and M. S. Balakrishna, *Eur. J. Inorg. Chem.*, 2018, 1707; (*e*) R. González-Fernández, P. Crochet and V. Cadierno, *Dalton Trans.*, 2020, **49**, 210; (*f*) R. González-Fernández, J. Borge, P. Crochet and V. Cadierno, *Molbank*, 2020, **2020**, M1110.

30 W. L. F. Armarego and C. L. L. Chai, in *Purification of Laboratory Chemicals*, Butterworth-Heinemann, Oxford, 5th edn, 2003.

31 V. Kumar, M. P. Kaushik and A. Mazumdar, *Eur. J. Org. Chem.*, 2008, 1910.

32 (*a*) V. Kumar, *Synlett*, 2005, 1638; (*b*) W. E. Luttrell, *J. Chem. Health Saf.*, 2009, **16**, 29.

33 (*a*) *CrysAlis^{Pro} CCD & CrysAlis^{Pro} RED*; Oxford Diffraction Ltd., Oxford, UK, 2008; (*b*) *CrysAlisPro: Data Collection and Processing Software for Agilent X-ray Diffractometers, XRD Products*, Agilent Technologies, Oxford, UK, 2013.

34 L. J. Farrugia, *J. Appl. Crystallogr.*, 2012, **45**, 849.

35 L. Palatinus and G. Chapuis, *J. Appl. Crystallogr.*, 2007, **40**, 786.

36 G. M. Sheldrick, *SHELXL97: Program for the Refinement of Crystal Structures*, University of Göttingen, Göttingen, Germany, 1997.

37 *International Tables for X-Ray Crystallography, Volume C*, ed. A. J. C. Wilson, Kluwer Academic Publishers, Dordrecht, The Netherlands, 1992.

38 M. Nardelli, *Comput. Chem.*, 1983, **7**, 95.

39 (*a*) V. Barone, M. Cossi and J. Tomasi, *J. Chem. Phys.*, 1997, **107**, 3210; (*b*) B. Mennucci and J. Tomasi, *J. Chem. Phys.*, 1997, **106**, 5151; (*c*) M. T. Cancès, B. Mennucci and J. Tomasi, *J. Chem. Phys.*, 1997, **107**, 3032; (*d*) V. Barone, M. Cossi and J. Tomasi, *J. Comput. Chem.*, 1998, **19**, 404; (*e*) J. Tomasi, B. Mennucci and M. T. Cancès, *J. Mol. Struct.: THEOCHEM*, 1999, **464**, 211; (*f*) G. Scalmani and M. J. Frisch, *J. Chem. Phys.*, 2010, 132, 114110.

40 (*a*) A. D. Becke, *Phys. Rev. A*, 1988, **38**, 3098; (*b*) C. Lee, W. Yang and R. G. Parr, *Phys. Rev. B*, 1988, **37**, 785; (*c*) A. D. Becke, *J. Chem. Phys.*, 1993, **98**, 5648; (*d*) P. J. Stephens, F. J. Devlin, C. F. Chabalowski and M. J. Frisch, *J. Phys. Chem.*, 1994, **98**, 11623.

41 W. J. Hehre, L. Radom, J. A. Pople and P. v. R. Schleyer, in *Ab Initio Molecular Orbital Theory*, Wiley, New York, 1986.

42 P. J. Hay and W. R. Wadt, *J. Chem. Phys.*, 1985, **82**, 270.

43 (*a*) H. B. Schlegel, *J. Comput. Chem.*, 1982, **3**, 214; (*b*) H. B. Schlegel, *Theor. Chem. Acc.*, 1984, **66**, 333; (*c*) X. Li and M. J. Frisch, *J. Chem. Theory and Comput.*, 2006, **2**, 835.

44 (*a*) C. Gonzalez and H. B. Schlegel, *J. Chem. Phys.*, 1989, **90**, 2154; (*b*) C. Gonzalez and H. B. Schlegel, *J. Phys. Chem.*, 1990, **94**, 5523.

45 (*a*) D. A. McQuarrie, in *Statistical Mechanics*, Harper and Row, New York, 1976; (*b*) F. Jensen, in *Introduction to Computational Chemistry*, 2nd Ed., John Wiley & Sons, Chichester, 2007; (*c*) C. J. Cramer, in *Essentials of Computational Chemistry: Theories and Models*, 2nd Ed., John Wiley & Sons, Chichester, 2013.

46 R. F. Ribeiro, A. V. Marenich, C. J. Cramer and D. G. Truhlar, *J. Phys. Chem. B*, 2011, **115**, 14556.

47 *Gaussian 09, Revision A.1*, M. J. Frisch, G. W. Trucks, H. B. Schlegel, G. E. Scuseria, M. A. Robb, J. R. Cheeseman, G. Scalmani, V. Barone, B. Mennucci, G. A. Petersson, H. Nakatsuji, M. Caricato, X. Li, H. P. Hratchian, A. F. Izmaylov, J. Bloino, G. Zheng, J. L. Sonnenberg, M. Hada, M. Ehara, K. Toyota, R. Fukuda, J. Hasegawa, M. Ishida, T. Nakajima, Y. Honda, O. Kitao, H. Nakai, T. Vreven, J. A. Montgomery, Jr., J. E. Peralta, F. Ogliaro, M. Bearpark, J. J. Heyd, E. Brothers, K. N. Kudin, V. N. Staroverov, R. Kobayashi, J. Normand, K. Raghavachari, A. Rendell, J. C. Burant, S. S. Iyengar, J. Tomasi, M. Cossi, N. Rega, J. M. Millam, M. Klene, J. E. Knox, J. B. Cross, V. Bakken, C. Adamo, J. Jaramillo, R. Gomperts, R. E. Stratmann, O. Yazyev, A. J. Austin, R. Cammi, C. Pomelli, J. W. Ochterski, R. L. Martin, K. Morokuma, V. G. Zakrzewski, G. A. Voth, P. Salvador, J. J. Dannenberg, S. Dapprich, A. D. Daniels, O. Farkas, J. B. Foresman, J. V. Ortiz, J. Cioslowski and D. J. Fox, Gaussian, Inc., Wallingford, CT, 2009.

48 (*a*) C. Riplinger and F. Neese, *J. Chem. Phys.*, 2013, **138**, 034106; (*b*) C. Riplinger, B. Sandhoefer, A. Hansen and F. Neese, *J. Chem. Phys.*, 2013, **139**, 134101.

49 (*a*) D. Andrae, U. Haeussermann, M. Dolg, H. Stoll and H. Preuss, *Theor. Chim.* Acta, 1990, **77**, 123; (*b*) F. Weigend and R. Ahlrichs, *Phys. Chem. Chem. Phys.*, 2005, **7**, 3297.

50 (*a*) J. L. Pascual-Ahuir and E. Silla, *J. Comput. Chem.*, 1990, **11**, 1047; (*b*) J. L. Pascual-Ahuir, E. Silla and I. Tuñón, *J. Comput. Chem.*, 1991, **12**, 1077; (*c*) J. L. Pascual-Ahuir, E. Silla and I. Tunón, *J. Comput. Chem.*, 1994, **15**, 1127; (*d*) T. N. Truong and E. V. Stefanovich, C*hem. Phys. Lett.*, 1995, **240**, 253; (*e*) V. Barone and M. Cossi, *J. Phys. Chem. A*, 1998, **102**, 1995.

51 T. J. Lee and P. R. Taylor, *Int. J. Quantum Chem.*, 1989, **36**, 199.

52 D. G. Liakos and F. Neese, *J. Chem. Theory Comput.*, 2015, **11**, 4054.

53 (*a*) E. J. Baerends, D. E. Ellis and P. Ros, *Chem. Phys.*, 1973, **2**, 41; (*b*) B. I. Dunlap, J. W. Connolly and J. R. J. Sabin, *Chem. Phys.*, 1979, **71**, 3396; (*c*) C. J. Van Alsenoy, *Comput. Chem.*, 1988, **9**, 620; (*d*) R. A. Kendall and H. A. Früchtl, *Theor. Chem. Acc.*, 1997, **97**, 158; (*e*) K. Eichkorn, O. Treutler, H. Öhm, M. Häser and R. Ahlrichs, *Chem. Phys. Lett.*, 1995, **240**, 283; (*f*) K. Eichkorn, F. Weigend, O. Treutler, R. Ahlrichs, *Theor. Chem. Acc.*, 1997, **97**, 119; (*g*) J. L. J. Whitten, *Chem. Phys.*, 1973, **58**, 4496.

54 F. Neese, *WIREs Comput. Mol. Sci.*, 2018, **8**, e1327.

55 (*a*) M. Dolg, H. Stoll and H. Preuss, *J. Chem. Phys.*, 1989, **90**, 1730; (*b*) F. Weigend, *J. Comput. Chem.*, 2008, **29**, 167.

56 A. Hellweg, C. Hattig, S. Hofener and W. Klopper, *Theor. Chim. Acta*, 2007, **117**, 587.

57 T. A. Keith, *AIMAll program, Version 10.12.11*, 2010.

View Article Online
DOI: 10.1039/D0CY00523A

For Graphical Abstract use only

The catalytic hydration of cyanamides to ureas has been accomplished employing, for the first time, homogeneous catalysts, *i.e.* the phosphinous acid complexes [$MCl_2(\eta^6$-*p*-cymene)(PMe_2OH)] (M = Ru, Os). The differences in reactivity found between cyanamides and classical organonitriles could be rationalized by means of computational chemistry calculations.